UNIVERSITY OF CAPE COAST

STATISTICAL MODELLING OF FERTILITY RATE OF GHANA

ASUAH ABDUL AZZIZ ATINGANE

2023

UNIVERSITY OF CAPE COAST

STATISTICAL MODELLING OF FERTILITY RATE OF GHANA

BY

ASUAH ABDUL AZZIZ ATINGANE

Thesis submitted to the Department of Statistics of the School of Physical Science, College of Agriculture and Natural Science, University of Cape Coast, in partial fulfilment of the requirements for the award of Master of Philosophy degree in Statistics

NOVEMBER 2023

DECLARATION

Candidate's Declaration

I hereby declare that this thesis is the result of my own original research and that no part of it has been presented for another degree in this university or elsewhere.

Candidate's Signature…… Date……

Name: Asuah Abdul Azziz Atingane

Supervisor's Declaration

I hereby declare that the preparation and presentation of the thesis were in accordance with the guidelines on supervision of thesis laid down by the University of Cape Coast.

Supervisor's Signature……. Date…….

Name: Dr. Arimiyaw Zakaria

ABSTRACT

The purpose of the study is to model the fertility rate of Ghana. The study is based on Ghana's fertility data that spans the years 2014 – 2020. Three standard fertility models – the Hadwiger, Gamma, and Beta model – are fitted to the data with the view of selecting the best model. The study shows that there were, on average, 332 live births per 100,000 women for the period 2014 – 2020. In the period, number of live births lingered between 41 per 1,000,000 women and 741 per 100,000 women. The results further show that the distribution of Ghana's fertility is positively skewed. A significant observation in the study is that there is, on yearly basis, continuous decline in the fertility rate of Ghana. Ghana's fertility is highest among women in the 25 – 30 reproductive ages. The study finds the Hadwiger model most suitable for modelling Ghana's fertility data. The results indicate that forecasted fertility rates for the years 2021, 2022, and 2023 appear to be higher than the actual ASFRs for the year 2020 for women below the age of about 30 years. The projected values show that there will be 393, 393, and 392 live births per 100,000 women for the respective years 2021, 2022, and 2023. In addition, for the period 2021 – 2023, the ASFRs of Ghana will continue to decline with highest fertility rate occurring among women in the 25 – 29 reproduction years. The study is of the view that Government and its agencies, the National Population Council, and other planners and policy makers adopts the Hadwiger fertility model in their quest to estimate various fertility rates of Ghana for planning and decision-making process. Also, the study recommends further investigation into factors that influence the decline in fertility rate of Ghana.

KEY WORDS

Age-Specific Fertility Rate

Beta Model

Fertility Models

Gamma Model

Hadwiger Model

Seasonal ARIMA

ACKNOWLEDGEMENTS

My foremost thanks go to Almighty God for His direction and security throughout the study. My sincere gratitude and appreciation go to principal supervisor, Dr. Arimiyaw Zakaria of the Department of Statistics, University of Cape Coast, for his guidance, constructive criticisms and suggestions that have led to the successful completion of this work.

I wish to acknowledge all lecturers of the Department of Statistics, University of Cape Coast, for their overwhelming support throughout the study.

I want to thank all my friends and love ones in and outside UCC. I wish to acknowledge the Samuel and Emelia Brew-Butler SGS/GRASAG, UCC Research Grant for their support. Finally, I want to express my profound gratitude to uncle, Abdulai Asuah, my parent and the entire family for their love, prayers, and support.

DEDICATION

To Asuah's family

TABLE OF CONTENTS

LIST OF TABLES

LIST OF FIGURES

LIST OF ABBREVIATIONS

ASFR *Age specific Fertility Rate*

GDHS *Ghana Demographic Health Services*

UN *United Nations*

PRB *Population Reference Bureau's*

GFR *General Fertility Rate*

TFR *Total Fertility Rate*

GHS *Ghana Health Services*

AIC *Akaike's Information Criteria*

AEM *Adjusted Error Model*

MACB *Mean Age of Childbirth*

NIPSSR *National Institute of Population and Social Security Research*

SFI *Synthetic Fertility Index*

SN *Skew Normal*

HBA *Hierarchical Bayesian Approach*

ML *Maximum likelihood*

CDFs *Cumulative Density Functions*

PDFs *Probability Density Functions*

PMFs *Probability Movement Functions*

ACF *Autocorrelation Function*

PACF *Partial Autocorrelation Function*

AR *Autoregressive*

MA *Moving Average*

ARIMA *Autoregressive Integrated Moving Average*

SARIMA *Seasonal Autoregressive Integrated Moving Average*

SSE *Sum of Square Error*

AICs *Corrected Akaike's Information Criteria*

GSS *Ghana Statistical Services*

CHAPTER ONE

INTRODUCTION

The chapter explores the background of the study. The background will introduce various works on fertility and its modelling, which are further examined in Chapter Two. Also, the chapter presents statement of the problem, objectives, significance of the study, geological context of the study area, description of the dataset used for the study, data analyses procedure and the study's organization.

Background to the Study

Population dynamics (i.e., how the population is distributed, its density, and its increase) is the focus of demography. Demography is a discipline that studies human population dynamics (Gebremeskel, 2016). A population's size (increase or decrease), composition, and spatial distribution are all influenced by five "demographic processes" – birthrates, mortality rates, migration patterns, social mobility, and marriage (Sharma, 2004). The most frequently cited example of a region where such demographic factors in general and fertility, in particular, have reached a plateau is Sub-Saharan Africa (or simply Africa) (Gebremeskel, 2016).

Having as many offspring as possible was a fundamental objective in ancient human communities. Ghana is not an exception to the trend of limiting and managing family size (Bosomprah, 2008). Despite the fact that fertility has decreased from 6.4 offspring to every woman in 1988 to 4.0 kids to a woman for 2008, fertility levels remain high when compared to the global average of 2.5 offspring per woman (Population Reference Bureau's [PRB], 2011). The

drop and differences cutting-edge infertility have been attempted to be explained. The five (5) phases of the Ghana Demographic Health Survey (GDHS) provide some insight; for example, contraceptive use was 5% in 1988, grew to 19% in 2003, and then slightly decreased to 17% in 2008 (Calverton, 2008). It is possible that contraception is not the primary reason for the decrease.

The transition in Sub-Saharan Africa to low fertility has garnered increasing focus in recent years. According to traditional hypothesis of demographic transition, considerable decrease in mortality have led to a decline in fertility. The drop in fertility has been slower in Africa than it has been elsewhere. According to the 2015 update of World Population Prospects (UN population Division, 2015), 1.3 billion of the 2.4 billion people that will be added to the world's population between 2015 and 2050 will reside in Africa. Physical access to health facilities is a crucial determinant of how people seek medical attention in distant places (Crissman et al., 2013; Gabrysch, Cousens, Cox & Campbell, 2011; & Sychareun, Hansana, Phengsayanh, Chaleunyong, & Tomson, 2015).

It is worth noting that within a demographic setting, fertility refers to the real production of children, as opposed to the physical ability to conceive, which is referred to as fecundity. Demographers have always measured a population increase as the rate with which fresh babies are born into the population (Akoth, 2017). Fertility is defined as the capacity to conceive and bear offspring, as well as the capability to get pregnant through sexual intercourse (Davis, 2021). According to Britannica, a person or a couple's ability to reproduce through regular sexual activity is term as fertility.

Demographers have been interested in modeling fertility data for a long time. To characterize the age-specific reproductive pattern, a range of numerical models have been developed. Most of these approaches have been demonstrated to suit one-year age-specific fertility rate curves of human societies extremely well (Hoem et al., 1981). For women of reproductive age, the typical fertility curve has a bell-shaped peak at age 25. Fertility is low from the age of 15, the beginning of reproductive age, rises among women mostly in 25 – 30 age category, subsequently starts to drop and has a really low value of fertility for women after the age of 35, and typically terminates somewhere at age of 49, the completion of reproductive age period (Srivastava, Singh, Pandey, & Narayan, 2021). Various reproductive measures and mathematical models have been presented in the literature to explain a process of human fertility rate (Visalakshi & Geetha, 2018). Theoretical distribution has been applied for years to predict fertility statistics and describe the reproductive patterns of women of childbearing age.

According to a UN study, nations are categorized into three groups based on the highest or peak age of fertility and the behavior of the fertility curve around the peak. As a result, there are three types of peak – early peak, late peak, and broad peak. When it comes to fertility, the early peak type reaches its peak between the years of 20 to 24, whereas the late peaks type reaches its peak between the ages 25 to 29. The wide peak type of the fertility level for age ranges 20 – 24 as well as 25 – 29 years varies little, yet each of the rates is much higher than the rates for younger and older age groups (Mitra, 1967).

In all human societies, there is a well-known pattern to the structure of age specific reproductive rates through time. Some industrialized countries'

fertility patterns deviate from the traditional bell curve. Using information from aggregated age specific fertility rates (ASFRs), further formulations have been developed to identify the fertility pattern. This group age specific birth rate is more trustworthy since numerical choice is typically evident throughout the ages of female data, and the additional benefit of this type of data is that it is readily available (Singh, Gupta, & Singh, 2015). For most people who utilize contraceptive techniques to manage their fertility level, the age trend of fertility follows a pattern of increasing until a certain age and then declining from that point on. The pattern is consistent throughout populations (or countries) and over time, as well as across different cultures.

Globally, all human groups have been discovered to exhibit the same pattern (Gupta & Pasupuleti, 2013). This is true despite the fact that various socioeconomic and living conditions of individuals have an impact on various features of the pattern of fertility, such as the age at which peak fertility is attained and the threshold of fertility at various ages. For example, it has been discovered that the age patterns of fertility among women in developing nations differ from the age pattern of fertility among women in developed countries, both in terms of the stage by which highest fertility happens then the degree of fertility at different ages. While examining the two situations, it was discovered that the characteristic pattern described above remained the same in both instances. That is, although numerous traits associated with fertility behavior vary across populations due to a variety of factors, human fertility behavior stays consistent around the world, as demonstrated by Gupta and Pasupuleti (2013). Marriage, postpartum amenorrhea, sexual activity, postpartum

insusceptibility are all fundamental elements influencing Ghana's reproductive rates (Ghana Statistical Service [GSS], 2014).

Reproductive success depends on the social and biological context, so fertility rates are critical in any society. The estimation of standard fertility measures and fertility modeling are the two stages of the fertility profile in the human population. Education, employment, religion, contraception use are socioeconomic variables of anticipated family size and are sources of difference within fertility (Visalakshi & Geetha, 2018).

According to Norville, Gomez, and Brown (2003), the fertility rates in Africa are among the highest in the world. There are various reasons for this high fertility rates. A high level of infant and child mortality and premature and general marriages are some of these causes, leading to childbirth that begins early and lasts throughout most of the reproductive life span. The tradition of polygamy encourages co-wives to compete for offspring, contributing to high fecundity in many African countries. Because marriage has such a tremendous social and cultural significance, it is also common, which also occurs early in life. As a result, pregnancy starts early and typically lasts the entire reproductive cycle. One rationale for high fertility rates in African nations, according to Caldwell (1980), is that the majority of the people live in remote areas and are less industrialized. Since most people live in the countryside, large families are seen as a positive.

Even though single women still give birth, marriage is the main gateway to parenting and pregnancy (Blanc & Grey, 2002). According to research, societies that marry young have a high fertility rate and begin birthing young (Westoff & Marco, 2003). The median age of marriage in Ghana has slightly

increased. According to GSS, Ghana Health Service [GHS], and International Coaching Federation [ICF] Macro (2009), the median age at first marriage for women between the ages of 25 and 49 increased over the past two decades, going from 18.1 to 19.8. This trend shows that marriage is occurring later in life. There are, nevertheless, significant social and regional disparities (GSS, 2014).

Fertility patterns have changed significantly everywhere in the world during the past few decades. Previously, there was a general increase in female fertility, with most pregnancies happening in the early stages of a woman's reproductive years. However, this tendency has now changed to one of delayed and low fertility (Misha & Upadhyay, 2019). Differences in accuracy criteria can, of course, be motivated by differences in the goal of curve fitting. For example, fertility estimates may not require the same level of precision in the representation of data structure as empirical studies; indeed, forecasting approaches may serve a distinct purpose.

Not only is it realistic to estimate fertility indicators like the Total Fertility Rate (TFR), General Fertility Rate (GFR), and Age Specific Fertility Rate (ASFR), but it is also feasible to anticipate and project fertility to aid estimates. Since the cohort component projection approach is based on the ASFR, it occupies a prominent position among fertility indicators (Srivastava et al., 2021). The process of selecting the best-fitting distribution function from a predefined family of distributions is referred to as fitting model optimization. In this field, judgment and skill are required. Akoth (2017) claims that the model selection, parameter estimates, and fit evaluation processes are frequently iterative and require multiple iterations of each stage.

Statement of the Problem

According to Oberhofer and Reichsthaler (2004), the analysis of reproductive behavior is crucial to long-term structural changes. As a consequence, if accurately measured and modeled will aid in several demographic policy implementations. Models such as the Gamma, the Beta, and the Hadwiger are often used to study fertility curves (Peristera & Kostaki 2007).

Work done by Bongaart (2015) indicates that the applications of age-specific models are limited due to the demanding nature of the data. Fertility rates affect the size, structure, and makeup of a population at any given period (Mathivanan, Ghani & Ghani, 2018). The study carried out by Mathivanan et al., (2018) shows that the best-fitted model for Peninsular Malaysia between 1996 to 2014 is the Hadwiger model. However, a survey from Gayawan and Ipinyomi (2009) revealed that models selected could reproduce the data more but are often most complex.

A study conducted by Nyarko (2012) revealed that the amount of schooling of the female teenager and their spouse, the female adolescent's work status, wealth position, and media exposure all had a substantial impact on adolescent fertility. These predictors of adolescent fertility in Ghana, as shown in the research, could be used to target teenage sexual and reproductive health education programs through successful social advertising.

Studies carried out locally only focused on the factors that affect fertility, the total fertility rate, the age specific fertility rate, and many other factors; they did not measure or model the fertility data according to different suggested models. On their part, Gayawan Adebayo, Ipinyomi and Oyejola, (2010) assert that in the literature, various fertility models are available to

capture the trends peculiar to industrialized countries. While tremendous work has gone towards lowering Africa's fertility rates, models defining fertility trends have remained unsolved. Thus, this study aims to fit three different models to the fertility data of Ghana in order to propose the best model for forecasting fertility levels in the country.

Objectives of the Study

The study aims at selecting a model that best fits the fertility data of Ghana. Specifically, the study seeks to:

1. review some standard fertility models;
2. explore Ghana's fertility pattern;
3. determine the model that best fits Ghana's fertility data; and
4. forecast the fertility of Ghana for the period 2021 – 2023.

Research Questions

In order to achieve the objectives of the study, the following research questions are posed:

1. What are some of the standard fertility models?
2. What is the pattern of Ghana's fertility?
3. What model best fits the Ghana's fertility data?
4. What are the future values of Ghana's fertility for the period 2021 – 2023?

Significance of the Study

The findings of this study contribute significantly to the literature on the fertility modeling, particularly in the Ghanaian context. In addition, Government and other policy makers may find this study insightful as it provides information as to the specific standard fertility models that fits Ghana's fertility and consequently, guide them towards employing the appropriate model for fertility forecasting in the country.

Moreover, findings from this study will provide planners and policy makers with possible roadmaps for determining how the population might grow, shrink, or stabilize over time. Finally, understanding the nature of the country's fertility will aid governmental planning and decision making.

Geological Context of the Study Area

On the shore of the Gulf of Guinea is Ghana, a nation in Western Africa. Ghana's is one of Africa's most powerful nations despite the small geographical size, in part because of abundant natural riches and in part since it's the first black African nation south of Sahara to attain freedom from colonial power (Fage, Davies, Maier & Boateng, 2021).

Land

Ghana is the nation in equatorial Africa that shares borders with Burkina Faso to the north, Togo to the east, the Atlantic Ocean to the south, and Cote d'Ivoire to the west. It is situated on the Gulf of Guinea shore (Fage et al., 2021).

Relief and drainage

Ghana has generally low relief, with heights often reaching 3000 ft (900 meters). The dissected peneplain, which spans the nation's southwestern, northwestern, and extreme northern regions, is composed of Precambrian rocks. A dissected peneplain is a land surface that has been worn down by deterioration to a basically flat plain, then raised and sculpted by erosion into mountains and valleys (about 540 million to 4 billion years old). The Paleozoic sediments (250-540 million years old), which make up most of the rest of the country, are assumed to lie on pre-existing rocks. With several limestone layers mixed, the Paleozoic deposits are primarily sandstone and shale. They reside in Volta Basin, a sizable region in the north-central part of the country where temperatures hardly ever get over 500 feet (150 meters). Lake Volta, a man-made lake that extends 3275sq mile into the country's central area behind the Akosombo Dan, occupies the basin (8500 sq km). narrow plateaus between 1000 and 2000 feet (300 and 600 meters) high, bordered by stunning scarps to the north and south, and to some extent, to the west, are created by the higher limits of the basin (Fage et al., 2021).

The most noteworthy ridges are the Kwahu (Mampong) scrap (refer to Kwahu Plateau) in the south as well as the Gambaga Scarp in the north. The majority of the drainage system is comprised of the Volta River basin, which also contains Lake Volta, the Black, White, and Oti rivers. The watershed of Kwahu Plateau, for instance, flows south directly into the ocean from the Pra, Ankobra, Tano, and some few minor rivers, cutting them off from the Volta drainage system. Ghana's only true natural lake, Bosumtwi, is situated in a meteorite impact side south of Kumasi in the country's south-central area and

has no outlet to the ocean. There are many lagoons along the shore, most of which are created at the entrances of small creeks (Fage et al., 2021).

Climate

Ghana's climate is mostly the result of the interaction of two air masses: hot, dry contental air mass that develop over the Sahara and a warm, moist maritime tropical air mas that rises over the South Atlantic. Due to the winds from their respective hemispheres, both air masses move toward the equator and collide near the Guinea Coast for several months every year.in western Africa, the southwest trade winds take maritime tropical air northward while the harmattan, or northeast wind patterns transport continental air southward. Periodic line squall precipitation occurs in the area where these air masses collide (Fage et al., 2021).

Figure 1: Current Map of Ghana with regions

Limitations to the Study

In Ghana, the main source of fertility data lies at the bosom of Ghana Health Service (GHS). The completeness of the data from many outlets of the GHS is problematic. Complete data on fertility were available for the years 2014 through 2020. This has necessitated the study to focus on the period, even though a much wider data coverage was desired in order to enhance the accuracy of the results. To this end, if the results of the study is affected, it may be as a result of data scarcity.

Organization of the Study

This thesis is organized under the following five-chapter headings: Introduction, Literature Review, Methodology, Results and Discussions, and Summary, Conclusions and Recommendations. Chapter One introduces the thesis. It presents the background of the study, statement of the problem, objectives, significance of the study, and the study's organization.

Chapter Two reviews literature related to the study. It presents an extensive review of existing literature on fertility and its significance, as well as factors affecting fertility rates. The chapter also providing critical empirical reviews on fertility model fitting and inference.

Chapter Three deals with methodological development. In particular, the review of some standard fertility models and their parameter estimations are provided. Likewise, critical exposition of the effect of the model parameters on fertility curves were outlined. Chapter Four focuses on the implementation of the fertility models with application to Ghana fertility data. Also, exposition on the data analysis and its implication.

Finally, Chapter Five summarizes the study, presents the conclusions and recommendations.

CHAPTER TWO

LITERATURE REVIEW

Introduction

The chapter presents review of literature relating to the study. It considers conceptual and theoretical reviews on fertility, and discusses generally the factors that affect fertility rates. In what follows, a conceptual review is presented.

Conceptual Review

In fact, one of three key demographic attributes that distinguish any population is fertility (mortality and migration makes up the other two features). In general, the fertility curve for females of reproductive age is bell-shaped, peaking around 25 years. Fertility begins slowly at the age of 15, which marks the start of reproductive age, peaks for females between the ages of 25 and 30, then begins to fall and has a shallow value for females over 35 years, then ceases typically at the age of 49, that marks the end of the range of childbearing.

Total fertility rates, crude birth rates, net reproduction rates, Age specific fertility rates, and gross reproduction rates, are examples of common measures of fertility rates. Fertility rates are used as a benchmark or indicator to characterize fertility performance in a community and can be period or cohort-based. At any point in time, the birth rate influences structure, composition, and the size of a population (Mathivanan et al., 2018).

The Significance of Fertility

The function that fertility curves perform now on the population forecasts, which is vitally aimed at administration development actions, is one of the many reasons why people are interested in them. It is via fertility that human beings can naturally replace themselves to survive on our planet (Chandiok et al., 2016). Fertility is essential since it is the most important determinant of population dynamics and growth (Moultrie et al., 2013). Fertility plays a crucial role in overcoming mortality in the context of population dynamics, so it's essential to keep this in mind.

Factors Affecting Fertility Rates

According to Norville, Gomez, and Brown (2003), Africa has some of the largest fertility rates globally. There are several variables that contribute to these high fertility rates. A high level of infant and child mortality and premature and general marriages are some of these causes, leading to childbirth that begins early and lasts throughout most of the reproductive life span. The tradition of polygamy encourages co-wives to compete for offspring, contributing to high fecundity in many African countries.

Marriage has a great social and cultural significance, and occurs early in human life. As a result, childbirth starts early and typically lasts the entire reproductive cycle. According to Caldwell (1980), one explanation for the high fertility rates in African countries is the fact that most people live in rural regions and are less industrialized. Since most people live in the countryside, large families are seen as positive.

Marriage/ Sexually

According to Aryee (1985), marriage is an agreement between a male and a female that creates an almost long-lasting legal or culturally accepted relationship. According to McDonald (1984), women's marital status impacts how long they can have children. He says that while marriage or publicity to sexual fusion is not an adequate inhibitor of fertility, it may be a required contributing element. Morocco's fertility reduction is primarily due to a rise in females' average stage of marriage (Ayad and Roudi, 2006). Even though unmarried women continue to give birth, marriage represents the predominant exposure to pregnancy and motherhood (Blanc and Grey, 2002). According to research, societies that marry young have a high fertility rate and begin birthing young (Westoff & Macro, 2003).

Age

The most critical element that affects fertility is the age of the female. A woman has all of her eggs at birth, but as she gets older, the egg supply decreases. The reduction is very slow with teenagers (just fewer oval get 'missed) but increases faster when females approach their semi thirties (several ovaries get 'gone' by the day). In addition, with the decrease in the quantity of oval accessible, their oval condition deteriorates as women age increases. As women age grows, their available oval diminishes in quantity and reliability, making it more difficult to conceive and more probable that they would miscarry (Fertilitynetworkuk, n.d).

Sexual intercourse timing and frequency

The interval connecting the beginning of one cycle and the beginning of the next for most women is 28 days. During a 28-day process, ovulation (the release of an egg from the ovary) happens on day 14. Depending on which day(s) in the cycle sexual activity takes place, a sperm may or may not fertilize that egg. The likelihood of becoming prenatal is minimal from the start but then rises within the eight (8) day. A woman's chances of becoming pregnant, increase if she has intercourse two days before ovulating (Fertilitynetworkuk, n.d).

Contraception

Increased contraception use has led to an increase in postpartum infertility in nations where nursing or abstinence is a long-term practice (Bongaarts, 2015). According to Ghana 2014 Demographic and Housing Survey (DHS), 22% of women of reproductive age use modern contraceptives. In order to promote gender equality and provide all women and teenagers more power, Goal 5 of the sustainable development goals (SDG-5) recognizes family planning as crucial strategy to help countries accomplish this goal (Dockalova, Lau, Barclay, and Marshall, 2016).

Additionally, a woman's educational level can have an impact on her recognition and utilization of current contraceptive procedures. Residence and educational attainment of a woman are the two most reliable indicators of her present usage of contraceptive among Ghanaian females (Aviisah et al., 2018).

Earlier pregnancy

When compared to partners that have never been pregnant, individuals who've already accomplished a pregnancy together (regardless of whether or not that pregnancy resulted in the delivery of a baby) are much more likely to become pregnant (Fertilitynetworkuk, n.d).

Length of subfertility

The chances of pregnancy decrease with the length of time that couples have been attempting to conceive. In this case, the chances of a couple getting pregnant in less than three years are virtually double that of a pair who has been trying for more than three years (Fertilitynetworkuk, n.d).

Abortion

Even though induced abortion is unlawful in Africa, it has emerged as a significant influence in reducing fertility (United Nations [UN], 2001). Owoo, Lambon-Quayefio and Onuoha (2019) argues that polygyny, Christian religious background, low education levels, higher household affluence, and lower parity and family size are all positively associated with abortion. The authors further stated that the size of the household, post-secondary education, and a woman's beliefs about the legality of abortion in the country appear to be the most significant predictors of safe abortions in Ghana.

Empirical Review

In a study by Hoem et al. (1981) on the experiments in modeling recent Danish fertility curves in Danish, the gamma and beta densities, as well as the

Coale-Trussell, cubic Spline, and Hadwiger functions, two polynomial kinds, and two of Brass' interactive techniques, and the Gompertz curve were fitted. In terms of providing all angles, the spline function was far superior to the others. The Hadwiger function came in second, followed by Coale-Trussell and gamma density. These functions were all well-suited to the information. The remaining procedures were less precise, though one of the polynomials suited nicely.

Mathivanan et al., 2018 undertook a study to determine the most appropriate mathematical model for Peninsular Malaysia's current age-specific fertility rate. From 1996 to 2014, fertility data from Peninsular Malaysia was fitted to 4 mathematical functions; Gompertz, Gamma, Beta, and Hadwiger. Following examinations of the four models, the Hadwiger model was determined to be the best fit mathematical model. There was a tendency toward the best-fitting mathematical model, which switched the Hadwiger function to the Beta function, with data from the early twenty-first century. From 1996 to 2007, they found the Hadwiger model to be the most accurate. Also, from 2009 to 2014, see a change from the Hadwiger to Beta function fitting the data best. As a result, the Beta model has a good chance of being the better mathematical function for Peninsula Malaysia's age-specific fertility rates in the twenty-first century.

Vähi's contribution to the field of fertility display in Estonian was published in 2017. His goal was to forecast fertility using a distribution adequate for defining fertility curves. For the observed years, neither the Hadwiger distribution nor the Gamma distribution provided a sufficient approximation. Beta distribution was found to be the best fit for describing the curves under study. The change in the distribution parameters was almost linear. The first

parameter's value was increasing, while the second parameter's value was decreasing. For this fact, the linear trend necessitates prudence when making long-term predictions.

Mishra, Singh and Singh (2017) proposed the Skewed-Logistic distribution function fertility model to fit India's age-specific fertility rate pattern. They argued that the model is relatively adaptable, and can be used to simulate a variety of fertility trends found in India's many states. The model's parameters were calculated using the nonlinear least-squares method. The proposed model fits nicely with the fertility pattern for practically every state in the country, according to the results of their study. A skew logistic model has the benefit of being able to take into account a variety of human reproductive patterns. It is appropriate for both unimodal and multimodal fertility schedules.

Gayawan et al., (2010), carried out a study on Modeling Fertility Curves in Africa. They aimed to propose a flexible parametric model that may accurately describe the different patterns of African countries' age-specific fertility curves. According to their findings, 11 of the 15 countries studied have the lowest AIC values for the AEM. This demonstrates that their model can reproduce empirical fertility statistics for African countries better than the other models examined. The model they suggested was shown to be the best fit for 11 of the 15 countries. The Quadratic Spline provides the best match for the three countries, while the Hadwiger model captures only one better.

Person age-specific fertility rate projection is an important forecasting problem. The parametric curves that describe the annual age-specific rates are predicted using a multivariate time series model. Their objectives were to reduce the number of dimensions, provide reasonably accurate short-term

fertility forecasts, and generate long-term fertility predictions that preserve the uniform form throughout the course of historical data. The majority of the data's patterns are represented by gamma curves. Thus, the fertility forecaster may concentrate on analyzing and projecting demographically significant numbers (SDACB, MACB, and TFR). With a few basic strategies, it is possible to predict how the fitted curves would differ from the age-specific rates. Despite their importance for short-term accuracy, these bias corrections have little long-term impact. Only a correlation between the standard error and the mean childbearing age was found to be statistically significant (Thompson, Bell, Long & Miller, 1989).

Peristera and Kostaki (2007) studied fertility in modern populations and proposed a new flexible model could describe both the old and new patterns of fertility. The proposed model fits both historical and cohort data best as compared to other models considered in their study, whereas Beta Model performed similarly well. The proposed model was considered superior to the Beta model since it had fewer parameters. The results further showed that Quadratic Spline models fit period data well, although they underestimated the tails of fertility curves in many circumstances. When it comes to cohort data, Spline fell short of the other models. For most of the datasets tested, both period and cohort data, the Hadwiger and Gamma models offered minor successful fits. However, the Gamma model performed better for Belgium's historical data (before 1990). Peristera and Kostaki further proposed a second model and its adjusted variant to describe populations with high early-age fertility. They found that both models produced successful fits of skewed fertility schedules equivalent to those provided by the Hadwiger mixture model. They indicated

that early-age fertility patterns were once restricted to a small number of predominantly English-speaking countries, but are now more evenly dispersed across Europe. Also, the design of first births in nations with high early-age fertility showed a pronounced peak in the younger age groups, even more, prominent than the pattern of total fertility.

Visalakshi & Geetha (2018), on the other hand, used fertility curves to simulate the age-specific fertility rate in India. By applying nonlinear models using Age-Specific Fertility Rate (ASFR) data for all Indian communities obtained as of the illustrated, their research attempts to look at the current pattern of ASFR as well as the trend in fertile age groups. Each of the five models has been equipped with the age-specific fertility rate, forward and backward age specific fertility rate for 2011 to 2015. For all models and states in 2012, the forward and backward age specific fertility rate were significant. In the cubic and compound models, states with age-specific fertility rates that stand out include Assam, Himachal Pradesh, Jharkhand, Kerala, and Odisha. Forward and backward age-specific fertility rates stood tall in 2014 than all other models. However, in the cubic and compound models, states like Assam, Gujarat, Himachal Pradesh, Kerala, Rajasthan, and Tamil Nadu are notable. Forward age-specific fertility rates and backward age-specific fertility rates for all models and states were significant in 2015. However, the cubic model had substantial impact on states like Andhra Pradesh, Chhattisgarh, Haryana, Karnataka, Madhya Pradesh, and West Bengal. In comparison to the age-specific fertility rate fitted model in all states and years, the forward and backward age-specific fertility rate yielded the best-fitting model.

Gupta and Pasupuleti (2013) conducted the study "a new behavioral model for fertility schedules", and introduced a new fertility model that is based on the generalization of logistic law. In addition to having excellent behavioral interpretation, the proposed model also has excellent parameter interpretations. In terms of goodness of fit, the model performs nearly as well as the other famous fertility distributions in the demographic literature, and it is nearly as efficient. The study's findings indicated that the fit of the suggested model is better than the fit of the Gompertz model, but the differences between the models are extremely slight. The projected model's fitness is insufficient for both the Hadwiger and the Gamma models. As a result, it can be said that the suggested model is successful in describing the fertility patterns of cohorts of Indian women and that the fit is excellent when compared to the fits of the other well-known fertility models that were taken into account in this research. The parameters of the proposed model, in contrast to those of previous models, have a demographic interpretation, which is a further benefit of the model. As a result, their model can be considered superior for modeling fertility schedules

In addition, Ramos, Peinado, Ollero, and Ramos (2013) conducted research in Spain on examining inequality in fertility curves fitted by gamma distributions. Their study sought to explain how partial orderings of distributions can be used to analyze fertility curves demographically. They assumed that increasing fertility rates among younger women would lead to a sustained increase in birth rates. In this case, the concentration of birth rates must rise, as well as the degree of inequality. However, a specific scenario arose in 1975–80 that would have gone unreported if simply the Synthetic Fertility Index (SFI) values were taken into account. Even though the latter index fell

from 1975 to 1996, inequality declined as expected from the Lorenz and modified Lorenz curves from 1975 to 1980. Concerning the total fertility rate, it reveals an unusual behavior pattern in the birth rate among younger women. The Synthetic Fertility Index (SFI) figures show that the fertility rate fell over this time while age-specific fertility rates rose.

Bermudez, Blanquero, Hernandez, and Planelles (2012) researched a fresh parametric classical aim that fit fertility curves. They offered a new parametric model based on two Weibull functions that provide age-specific fertility rates in their study. They also provided a specific example of the novel model for fitting fertility curves with the typical shape, free of distortion due to high early-age fertility. Even though the ideal might fit the 'classical' fecundity graphs, they display that, simplified typical per fewer parameters produces acceptable results. Except for Ireland data for 1995 and 1999 and Spain data for 2000, the numerical findings demonstrate that the novel technique offers the greatest match for each data-sets evaluated. Although alternative models, such as Hadwiger for Spain and Peristera-Kostaki for Ireland, gave better fits for these nations' data, a closer look at the data for these two countries shows that the mounted Weibull combination proved to provide a better match. The proposed model, on average, performs worse than models with more factors, with the Beta function as an exception, that serves poorer while having the most parameters (5). In most cases, the Peristera-Kostaki model provides the best fit. Even though not one model can provide the paramount fitting cutting-edge every situation, in their case they developed groups of novel normal aimed at suitable delivery towards practical age-specific fertility rates.

Melkersson and Rooth (2000) proposed a flexible count data model that accurately represents observed fertility patterns. Results of the study indicated that all models properly estimate roughly 40% to 80% of the sample observations if they allow for plus one margin of error. The Gamma model, which was employed as the parent distribution, accounted for individual heterogeneity, which can be read as time-dependent hazards between births. Melkersson and Rooth argued that some data are consistent with positive length dependence between births, which is in line with the finding from the dynamic modeling of fertility. As a result, the Poisson model was replaced by the more comprehensive Gamma model. They concluded that the data are conditionally under distributed, which is consistent with dynamic modeling findings of positive length dependency in underlying waiting times.

Mathematical Curves were used by Singh et al. (2015) to analyze fertility patterns among women in Uttar Pradesh. They modify the third-degree polynomial with respect to female age (Model I) to described the age specific fertility pattern of Uttar Pradesh. The authors proposed another model based on third degree polynomial with respect to the reciprocal of female age (Model II). They indicated that using a third-degree polynomial with the inverse of female age provides the best estimate of ASFR and adequately explains data variability. They found that Model I cannot get an acceptable forecast value for the age range 40 – 45 years, whereas Model II can get justified estimated ASFR values for this age range. They further found Model II to have high explanatory power and may be used to figure out how female fertility changes as females get older. They stated that the application of Model II is not restrict to ASFR estimates at the state level, but used to calculate ASFR for a residential dividend location.

Bongaarts (2015) did a study on estimating the proximate determinants' impact on fertility. The Bongaarts proximal element's function is fine-tuned in his work in light of fresh facts, research, and statistics that have been accessible over the last three decades. As evidenced by a higher accuracy in forecasting TFR in a set of 36 countries with current DHS surveys, the revised version model gives an enhanced assessment of the roles of the proximate drivers. The updated model's aggregate version is derived directly from the age-specific model, which provides a more solid analytic foundation for evaluating the fertility impact of the proximate factors. This is especially true for applications to sub-national populations (e.g., educational attainment or urban-rural divides), where age structures might differ significantly.

Srivastava et al. (2021) reviewed studies in modeling recent Indian fertility patterns. They presented models which were extensions of the Gompertz model, P-K Model, Gupta and Pasupuleti model, and the generalized skew-normal function. They found that their proposed functions are extremely flexible and are capable of producing a tight fit to the observed fertility. All the presented models were more functional, in terms of goodness-of-fit, than the initial ones examined for reproductive patterns in India and its states. The demographic explanation of the model's parameters were also addressed in their article, among other things. When the variables are interpreted from a demographic perspective, it is evident that Indian states have a far more diverse population profile than the United States.

Gebremeskel (2016) examined ASFRs at the country and regional level in Ethiopia and proposed a model that best represents various ASFR forms at the national and regional levels The performance of the model was then

compared to several current models. A hierarchical Bayesian approach was used to fit the suggested model, and this approach showed to be sufficiently versatile for local estimates compared to the standard formula, where estimates may be quite imprecise due to small sample sizes. Preliminary results of his study showed that Skew Normal (SN) has the lowest Akaike Information Criterion (AIC) values of any model tested. Based on Ethiopian and regional empirical fertility statistics, their suggested model outperformed each other existing model in six of eleven regions. Many posterior means were found to be closer in value to the genuine fixed fertility values, as demonstrated by the HBA results. As a result, they were more accurate and less uncertain than the other methods, like ML and Bayesian estimate equivalents. There is a consensus that HBA is the best method for this type of data because it is more consistent and precise (the low uncertainty). The study concluded that the suggested model was better at capturing the ASFR pattern at the national and regional levels than the other common models that were evaluated (Gebremeskel, 2016).

Chapter Summary

This chapter has examined relevant materials for the topic under examination for key facts and findings that have previously been established by earlier researchers, practical textbooks, websites, and other trustworthy sources. There is a question about whether Ghana's fertility statistics fit the various fertility models in the literature. As a result, this research aims to evaluate and provide Ghana's fertility statistics using three distinct models with the view of selecting the best model for estimating fertility levels in the country.

CHAPTER THREE

RESEARCH METHOD

Introduction

The theory of the models to be utilized, formulations, and techniques for assessing the available data to meet the study's objectives are presented in this chapter. It focuses on a precise and in-depth knowledge of the source of data, general fertility measurement, the mean age of women at childbirths, standard fertility models, the concept of time series analysis, and the model performance measures.

Age-Specific Fertility Rate

There are several measurements of fertility rate, but the study employs the age-specific fertility rate (ASFR). Age-specific fertility rate is the number of live births to a specific age or age interval divided by the midyear population in that age or age interval per 1000 women. Mathematically, ASFR can be obtained as:

$$ASFR = \frac{B_X}{W_X} \times 1000$$

where, B_X denotes the number of live births born to a specific age X, and W_X represents the midyear population corresponding to the age X. The ASFR often provides some additional insight as it can be computed for very short age intervals. The age pattern of fertility can, therefore, be represented by continuous density functions.

Mean Age of Women at Childbirths

A woman's average childbearing age is when she gave birth to her first child if she had been subjected to the age-specific fertility rates recorded in a given year throughout her life. The following formula can be used to calculate the average age at childbearing if the data is provided in five-year age groupings.

$$MACB = \frac{\sum af_a}{\sum f_a}$$

where, a is the mid-point for each age interval, and f_a is the age-specific fertility rate.

Alternatively, if the data is provided in the specific ages of the mothers, then it can be obtained as:

$$MACB = \frac{\sum (y+0.5) f_y}{\sum f_y}$$

where y denotes the age of mothers at child birth, and f_y is the age-specific fertility rate at age y.

Some Standard Fertility Models

The standard fertility models considered in this study are the Hadwiger model, Gamma and Beta models. A theoretical review of these is presented in this section.

The Hadwiger model

The Hadwiger model is written as

$$f(y)=\frac{ab}{c}\left(\frac{c}{y}\right)^{\frac{3}{2}}\exp\left[-b^2\left(\frac{c}{y}+\frac{y}{c}-2\right)\right]$$

where, *a*, *b*, and *c* are the parameters of the model. The height of the curve of the Hadwiger model is influenced by the parameter b. The mothers' average age is represented by the parameter c. The expression $\frac{ab}{c}$, on the other hand, refers to the maximum age-specific fertility rate and *a* is the total fertility rate, y represents the ages of mothers.

Estimation of the parameters of the Hadwiger model

Since the parameter *a* is the total fertility rate, it is regarded as a constant and would not be estimated. The other parameters, *b* and *c*, are estimated based on the method of maximum likelihood. The likelihood function is given as

$$L(y)=\prod_{i=0}^{m} f(y) \tag{1}$$

Making use of the Hadwiger model, we obtain

$$L(y)=\left(\frac{ab}{c}\right)^{m}\prod_{i=0}^{m}\left(\frac{c}{y}\right)^{\frac{3}{2}}\exp\left[-b^2\sum_{i=0}^{m}\left(\frac{c}{y}+\frac{y}{c}-2\right)\right]$$

Taking the natural log of the likelihood function gives

$$l(y)=\ln\left[\mathrm{L}(y)\right]=m\ln(ab)-m\ln(c)+\frac{3}{2}\sum_{i=0}^{m}\ln\left(\frac{c}{y}\right)-b^2\sum_{i=0}^{m}\left(\frac{c}{y}+\frac{y}{c}-2\right) \tag{2}$$

To estimate the parameter b, we take the partial derivative of Equation (2) with respect to *b*, and setting the result of the derivative to zero. This gives

$$\frac{\partial l(y)}{\partial b}=\frac{m}{b}-2b\sum_{i=0}^{m}\left(\frac{c}{y}+\frac{y}{c}-2\right)=0$$

Implies,

$$\frac{m}{b} = 2b\sum_{i=0}^{m}\left(\frac{c}{y}+\frac{y}{c}-2\right)$$

$$\frac{m}{b} = 2bc\sum_{i=0}^{m}\frac{1}{y}+\frac{2b}{c}\sum_{i=0}^{m}y-4mb$$

Making b^2 the subject gives

$$b^2 = \frac{m}{2\sum_{i=0}^{m}\left(\frac{c}{y}+\frac{y}{c}-2\right)} \tag{3}$$

Similarly, to estimate the parameter c, we have

$$\frac{\partial l(y)}{\partial c} = -\frac{m}{c}+\frac{3}{2}\sum_{i=0}^{m}\frac{1}{c}-b^2\sum_{i=0}^{m}\left(\frac{1}{y}-\frac{y}{c^2}\right)=0$$

Implies,

$$-\frac{m}{c}+\frac{3m}{2c}-b^2\sum_{i=0}^{m}\left(\frac{1}{y}-\frac{y}{c^2}\right)=0$$

And,

$$\frac{m}{2c}-b^2\sum_{i=0}^{m}\left(\frac{1}{y}-\frac{y}{c^2}\right)=0$$

Making b^2 the subject gives

$$b^2 = \frac{m}{2c\sum_{i=0}^{m}\left(\frac{1}{y}-\frac{y}{c^2}\right)} \tag{4}$$

Substituting Equation (4) into Equation (3),

$$\frac{m}{2c\sum_{i=0}^{m}\left(\frac{1}{y}-\frac{y}{c^2}\right)} = \frac{m}{2\sum_{i=0}^{m}\left(\frac{c}{y}+\frac{y}{c}-2\right)}$$

Implies,

$$\frac{1}{c\sum_{i=0}^{m}\frac{1}{y}-\frac{1}{c}\sum_{i=0}^{m}y} = \frac{1}{c\sum_{i=0}^{m}\frac{1}{y}+\frac{1}{c}\sum_{i=0}^{m}y-2m}$$

That is,

$$c\sum_{i=0}^{m}\frac{1}{y}+\frac{1}{c}\sum_{i=0}^{m}y-2m=c\sum_{i=0}^{m}\frac{1}{y}-\frac{1}{c}\sum_{i=0}^{m}y$$

Reduces to

$$\frac{2}{c}\sum_{i=0}^{m}y=2m$$

Making c the subject yields

$$c=\frac{1}{m}\sum_{i=0}^{m}y=\bar{y} \tag{5}$$

Substituting Equation (5) into Equation (4),

$$b^2=\frac{m}{2\bar{y}\sum_{i=0}^{m}\left(\frac{1}{y}-\frac{y}{\bar{y}^2}\right)}$$

Implies,

$$b^2=\frac{m}{2\bar{y}\sum_{i=0}^{m}\frac{1}{y}-\frac{2}{\bar{y}}\sum_{i=0}^{m}y}$$

That is,

$$b^2=\frac{m}{2\bar{y}\sum_{i=0}^{m}\frac{1}{y}-2m}$$

Making b the subject,

$$b=\sqrt{\frac{m}{2\bar{y}\sum_{i=0}^{m}\frac{1}{y}-2m}}$$

(6)

Hence, Equations (5) and (6) are the maximum likelihood estimators of the parameters of the Hadwiger model.

Assessing the effects of the parameters on the graph of the Hadwiger Model

The effects of the parameters on the graph of the Hadwiger model is assessed using ASFR data of Ghana from 2014 to 2020. A typical curve for the Hadwiger fertility model based on the data is presented in Figure 2.

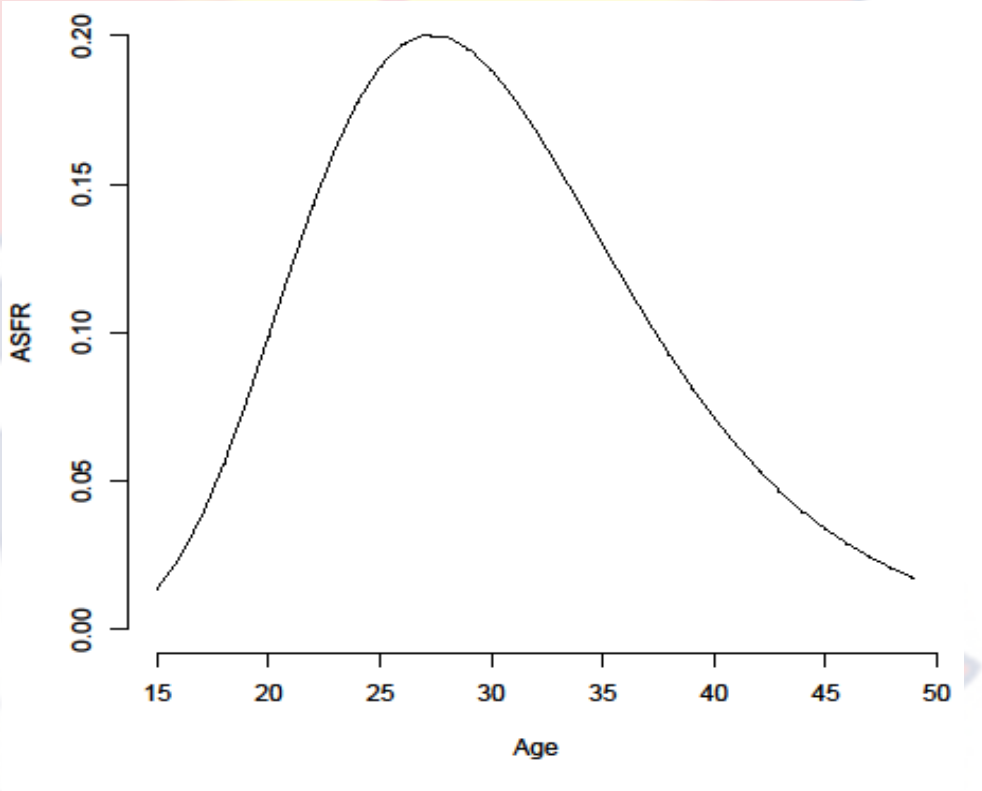

Figure 2: Plot of a typical Hadwiger age specific fertility rate curve.

It is clear that age-specific fertility rate rises quickly in the early ages, reaches its peak in the Middle Ages (25 to 30), and then declines gradually as people get older and stop having children.

The effect of the parameter *a* is examined in Figure 3.

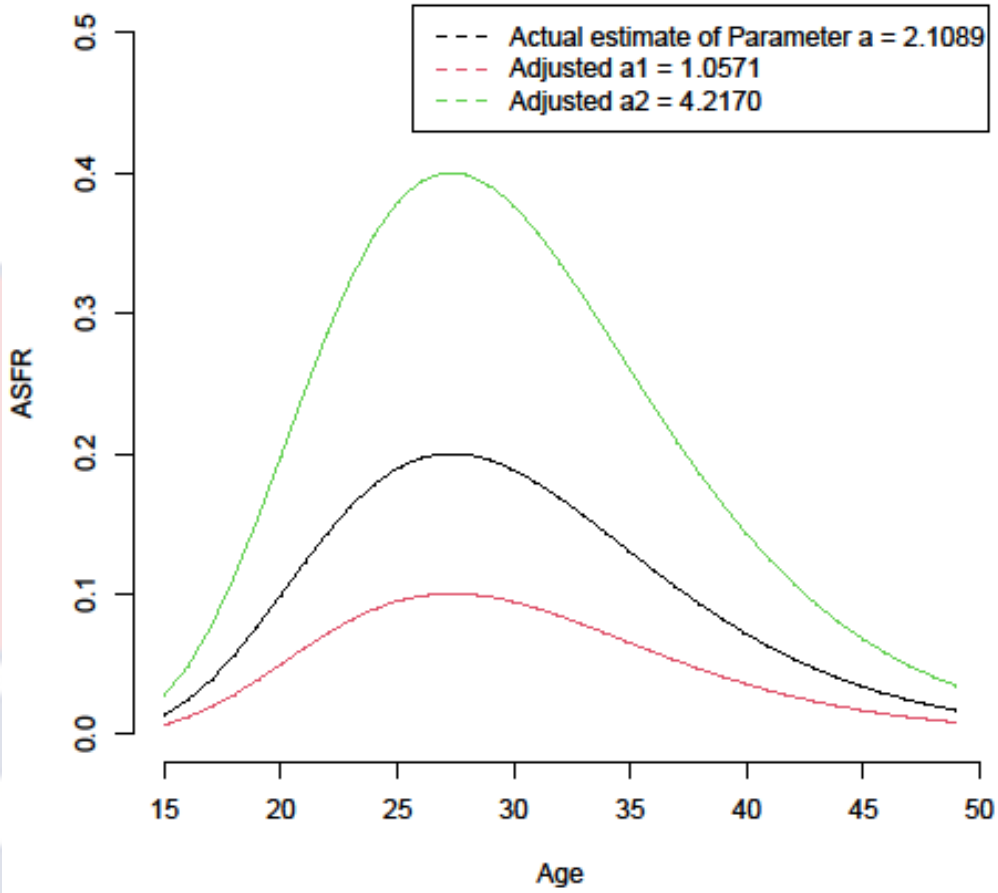

Figure 3: Plot of Hadwiger fertility curves for the parameter a at different levels.

On one hand, as the value of the parameter *a* decreases, the total area under the fertility curve reduces. On the other hand, as the value of the parameter *a* increases, the area under the curve increases. This shows that, indeed, the parameter *a* influences the total fertility rate of the distribution.

The influence of the parameter *b* is assessed in Figure 4.

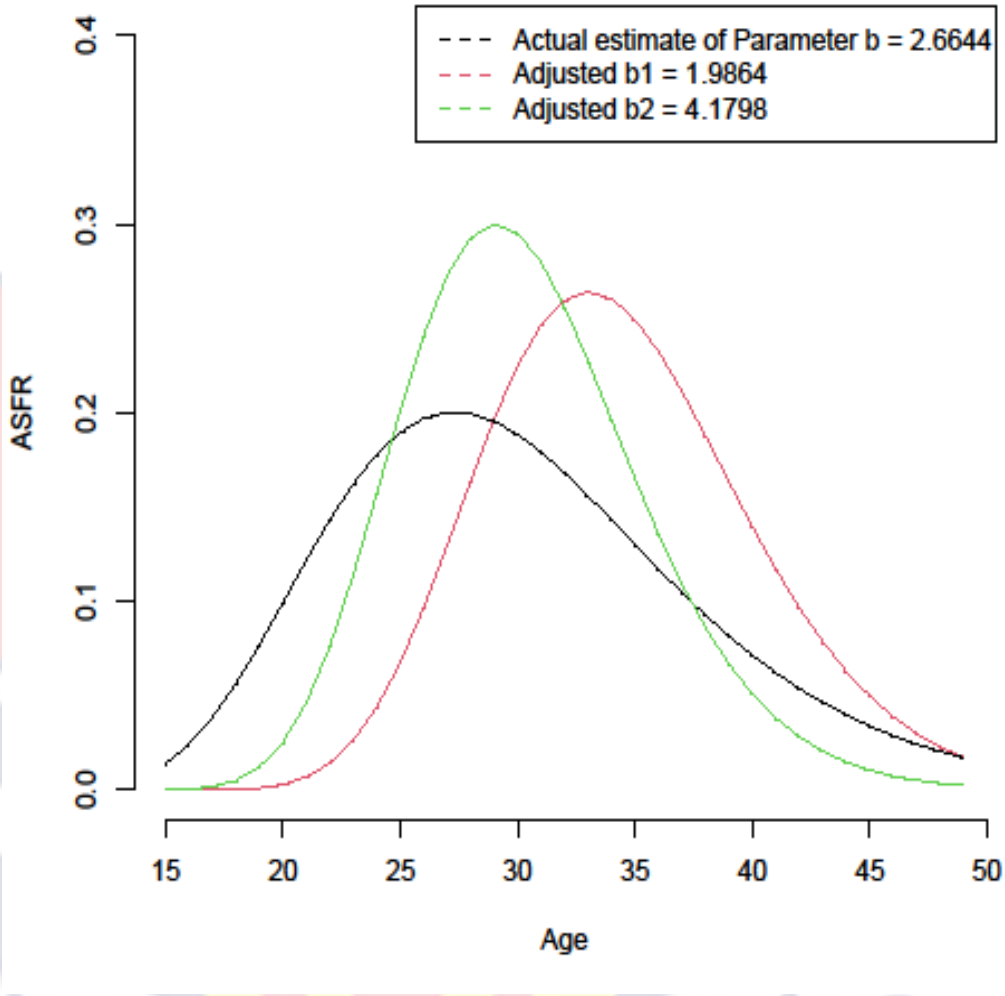

Figure 4: Plot of Hadwiger fertility curves for the parameter b at different levels.

The figure shows that as the value of the parameter *b* rises, the peak of the curve becomes somewhat moderate, reflecting a normal distribution.

Figure examines the effect of the parameter *c* on the Hadwiger fertility curve.

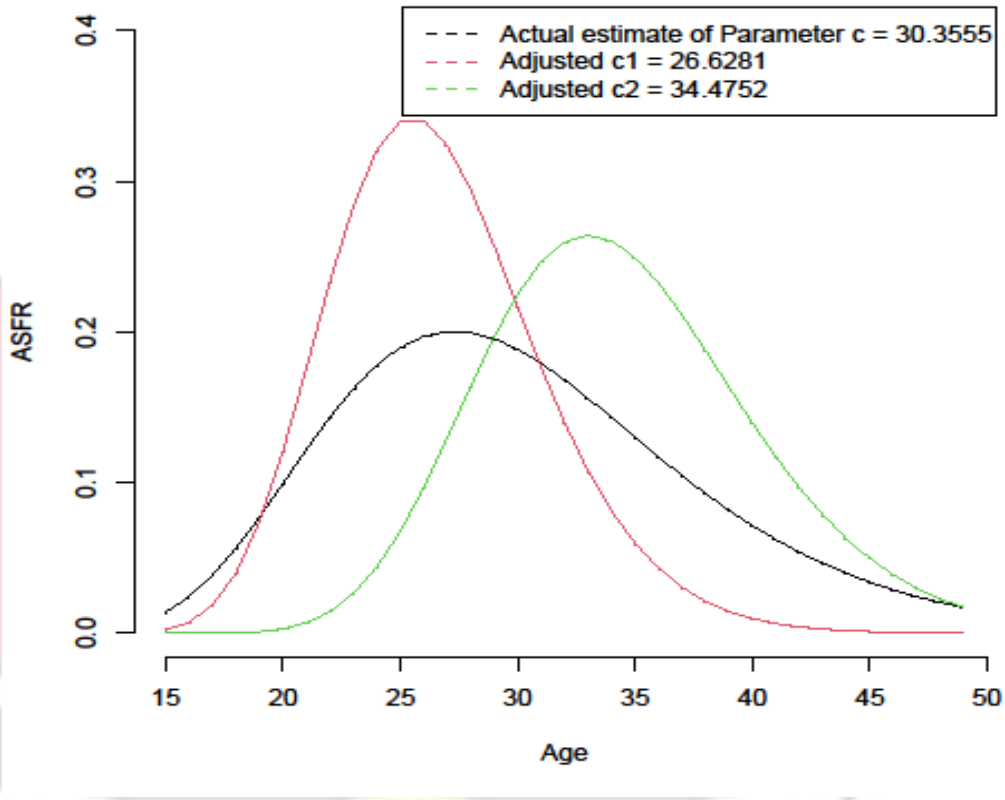

Figure 5: Plot of Hadwiger fertility curves for the parameter c at different levels.

The figure shows that as the value of the parameter *c* increases, the curve generally shifts to the right. This is indicative that the parameter *c* is a location parameter, and provides the approximate age interval of women within which maximum fertility occurs. When mothers are on average 26.6281 years old, the peak of the curve rises and shifted to the left-hand side; however, when mothers are on average 30.3555 years old, the peak of the curve also flattens out and becoming symmetric. The curve likewise reveals a sharp reduction with a mean age of 26.6281 years and increase in the proportion of women from the early to the maximum. There are more women in the old stage of reproduction when the mean age of mothers rises to 34.4752 years.

The Gamma fertility model

The Gamma fertility model can be expressed as:

$$f(y) = R\frac{1}{\Gamma(b)c^b}(y-d)^{b-1}\exp\left\{-\frac{(y-d)}{c}\right\} \text{ for } y > d$$

The parameter R influences the level of fertility, whereas the parameter d indicates the lowest age at childbirth. The parameters b and c are said to be connected to the function's mode, mean, and variance, but not in a straightforward linear fashion (Hoem et al., 1981).

Estimation of the parameters of the Gamma fertility model

The parameter *R* (which is a function of the total fertility rate), and parameter *d* (minimum age at childbirth) are treated as constants since they can be obtained directly from the fertility data, and need not be estimated. Other parameters in the model are estimated via the method of maximum likelihood. Using Equation (1), the likelihood function of the Gamma fertility distribution is given as

$$L(y) = \left(R\frac{1}{\Gamma(b)c^b}\right)^m \prod_{i=0}^{m}(y-d)^{b-1}\exp\left\{-\frac{1}{c}\sum_{i=0}^{m}(y-d)\right\}$$

Taking the natural logarithm of the likelihood function gives

$$l(y) = \ln\left[L(y)\right]$$
$$= m\ln R - m\ln\Gamma(b) - mb\ln c + (b-1)\sum_{i=0}^{m}\ln(y-d) - \frac{1}{c}\sum_{i=0}^{m}(y-d)$$

We first estimate the parameter b, by taking the partial differential of the ln likelihood function with respect to *b*, and setting the result to zero. That is,

$$\frac{\partial l(y)}{\partial b} = -m\psi(b) - m\ln c + \sum_{i=0}^{m}\ln(y-d) = 0 \qquad (7)$$

where $\psi(b) = \frac{\partial}{\partial b}\left[\ln\Gamma(b)\right]$ is a digamma function.

Secondly, we estimate parameter c, by taking the partial differential of the ln likelihood function with respect to *c*, equating the result to zero. Thus,

$$\frac{\partial l(y)}{\partial c} = -\frac{mb}{c} + \frac{1}{c^2}\sum_{i=0}^{m}(y-d) = 0$$

Making c the subject, we have

$$c = \frac{\sum_{i=0}^{m}(y_i - d)}{bm}$$

Alternatively,

$$c = \frac{\bar{y} - d}{b} \tag{8}$$

From Equation (7), making the digamma function the subject gives

$$\psi(b) = \frac{1}{m}\sum_{i=0}^{m}\ln(y-d) - \ln c \tag{9}$$

Substitute Equation (8) into Equation (9), we have

$$\psi(b) = \frac{1}{m}\sum_{i=0}^{m}\ln(y-d) - \ln\left(\frac{\bar{y}-d}{b}\right)$$

Grouping like terms together,

$$\psi(b) + \ln\left(\frac{\bar{y}-d}{b}\right) = \frac{1}{m}\sum_{i=0}^{m}\ln(y-d)$$

That is,

$$\psi(b) + \ln(\bar{y}-d) - \ln b = \frac{1}{m}\sum_{i=0}^{m}\ln(y-d)$$

Implies,

$$\psi(b) - \ln b = \frac{1}{m}\sum_{i=0}^{m}\ln(y_i - d) - \ln(\bar{y}-d) \tag{10}$$

But the digamma function is equivalent to the expression (Abramowitz & Stegum, 1964; Weisstein, 2002)

$$\psi(b) = \ln b - \frac{1}{2b} \tag{11}$$

Substituting Equation (11) into Equation (10),

$$\ln b - \frac{1}{2b} - \ln b = \frac{1}{m}\sum_{i=0}^{m} \ln(y-d) - \ln(\bar{y}-d)$$

That is,

$$-\frac{1}{2b} = \frac{1}{m}\sum_{i=0}^{m} \ln(y-d) - \ln(\bar{y}-d)$$

Making b the subject,

$$b = \left[\frac{2}{m}\sum_{i=0}^{m} \ln(y_i - d) - 2\ln(\bar{y}-d)\right]^{-1}$$

Equivalently,

$$b = \left[\frac{2}{m}\ln m + \frac{2-2m}{m}\ln(\bar{y}-d)\right]^{-1} \tag{12}$$

Substituting Equation (12) into Equation (8),

$$c = \frac{\bar{y}}{\left[\frac{2}{m}\ln m + \frac{2-2m}{m}\ln(\bar{y}-d)\right]^{-1}}$$

Alternatively,

$$c = \bar{y}\left[\frac{2}{m}\ln m + \frac{2-2m}{m}\ln(\bar{y}-d)\right] \tag{13}$$

Thus, Equations (12) and (13) are the maximum likelihood estimators of the parameters, b and c, of the Gamma fertility model.

Assessing the effect of the parameters of the Gamma model

To assess the effect of the parameters of the Gamma model, the study utilized the fertility of Ghana for the period under consideration. The Gamma fertility curve for the data is presented in Figure 6.

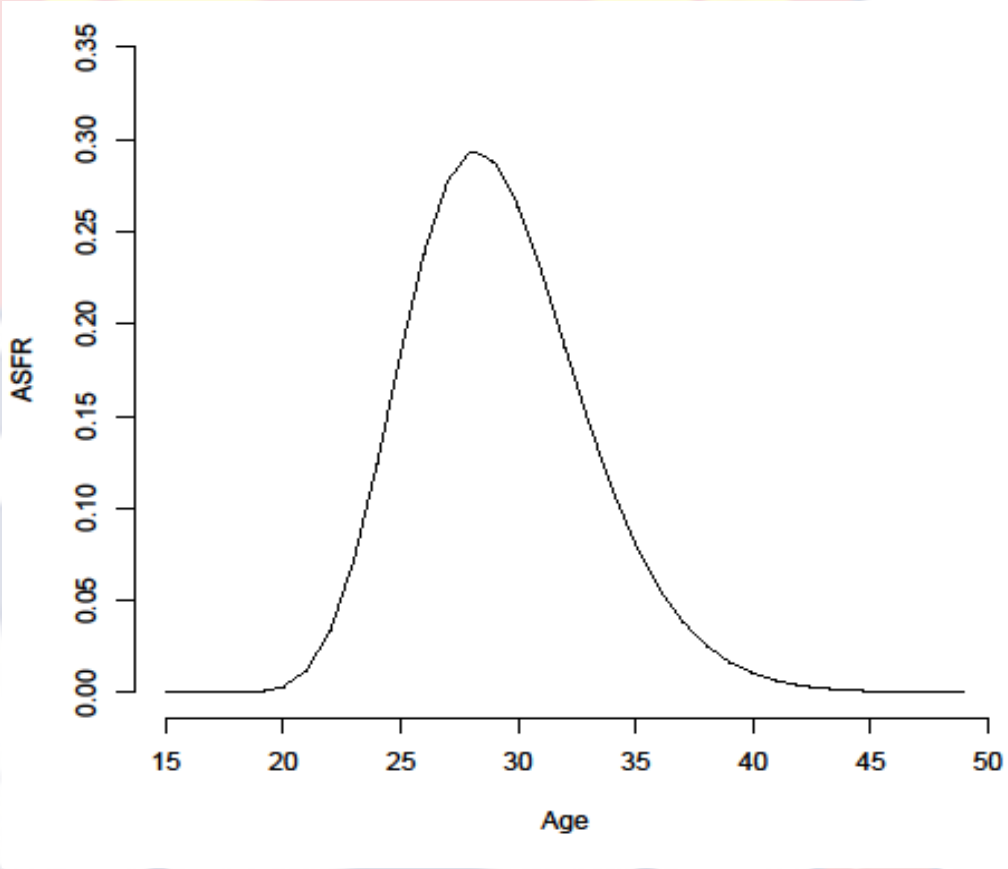

Figure 6: Gamma fertility curve of ASFR of Ghana, 2014 – 2020.

It is clear that the age specific fertility rate was low for ages (15 to 20), then rises quickly to its peak in the ages (27 to 30), and then declines gradually as people get older and stop having children.

The influence of the parameter *R*, which is related to total fertility rate, on the Gamma fertility curve is examined. The results are displayed in Figure 7.

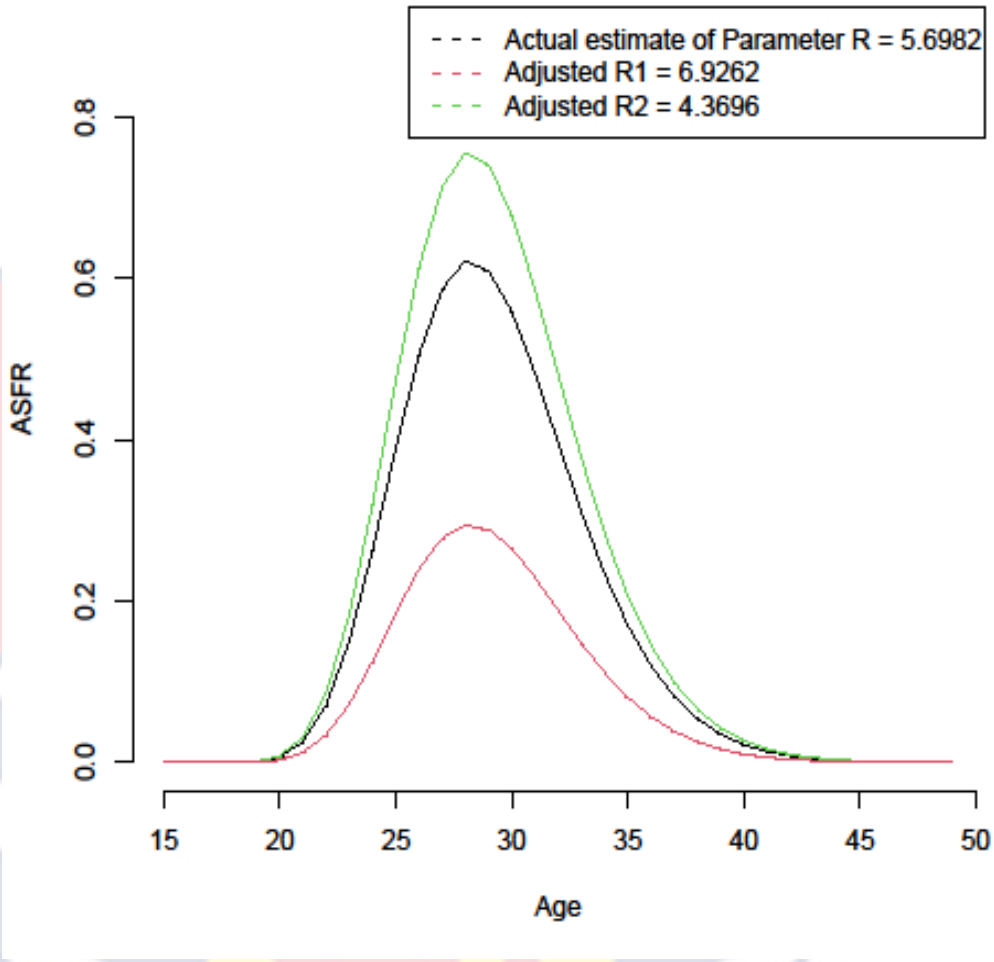

Figure 7: Gamma Fertility curves for different values of the parameter R.

The figure reveals that as the total fertility rate falls in value, the peak of the curve rises and becomes narrow; whereas as the total fertility rate rises, the peak of the curve decreases and tends to broaden.

The effect of the parameter b on the Gamma fertility curve is demonstrated in Figure 8.

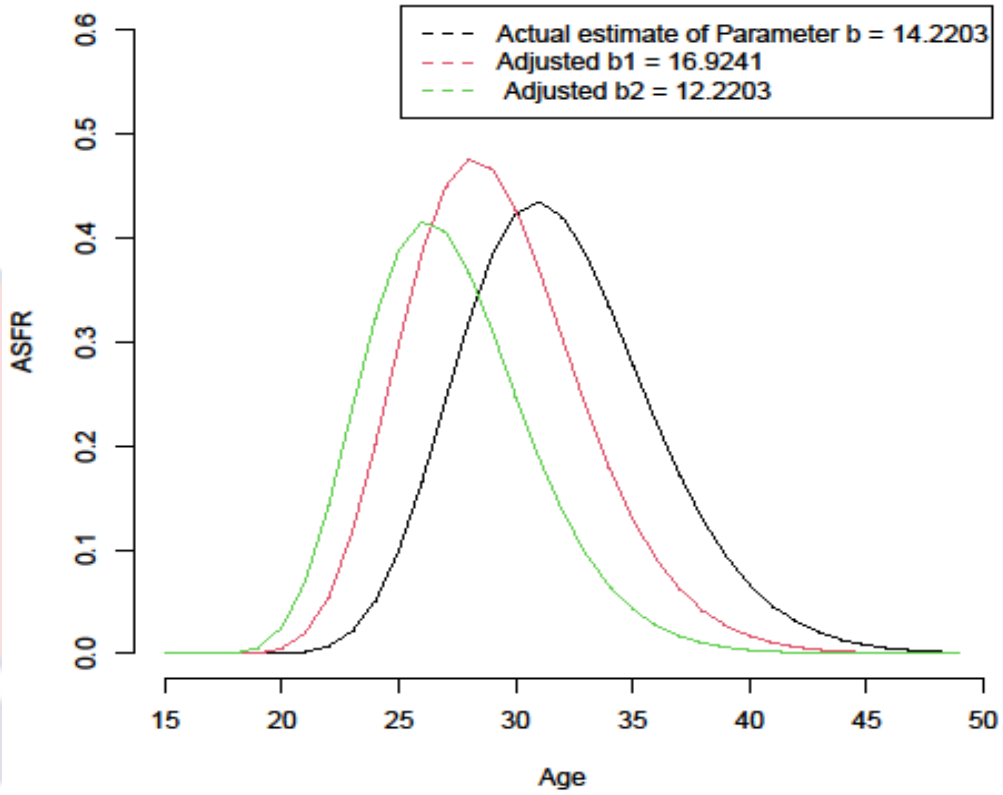

Figure 8: Gamma fertility curves for the parameter b at different levels.

It is evident from the figure that for the value of parameter at 14.2303, the Gamma fertility curve is more symmetric with its peak around the age 31 years. However, when the value increases to 16.9241, the curve tends to skew a bit to the left with highest ASFR peaks at age 27. Again, when the value falls to 12.2203, the curve tends to skew even more to the left with low ASFR values peaks at age 25 years. Thus, the parameter *b* affects the symmetry of the Gamma fertility curve.

The effect of the parameter *c* on the Gamma fertility curve is highlighted in Figure 9.

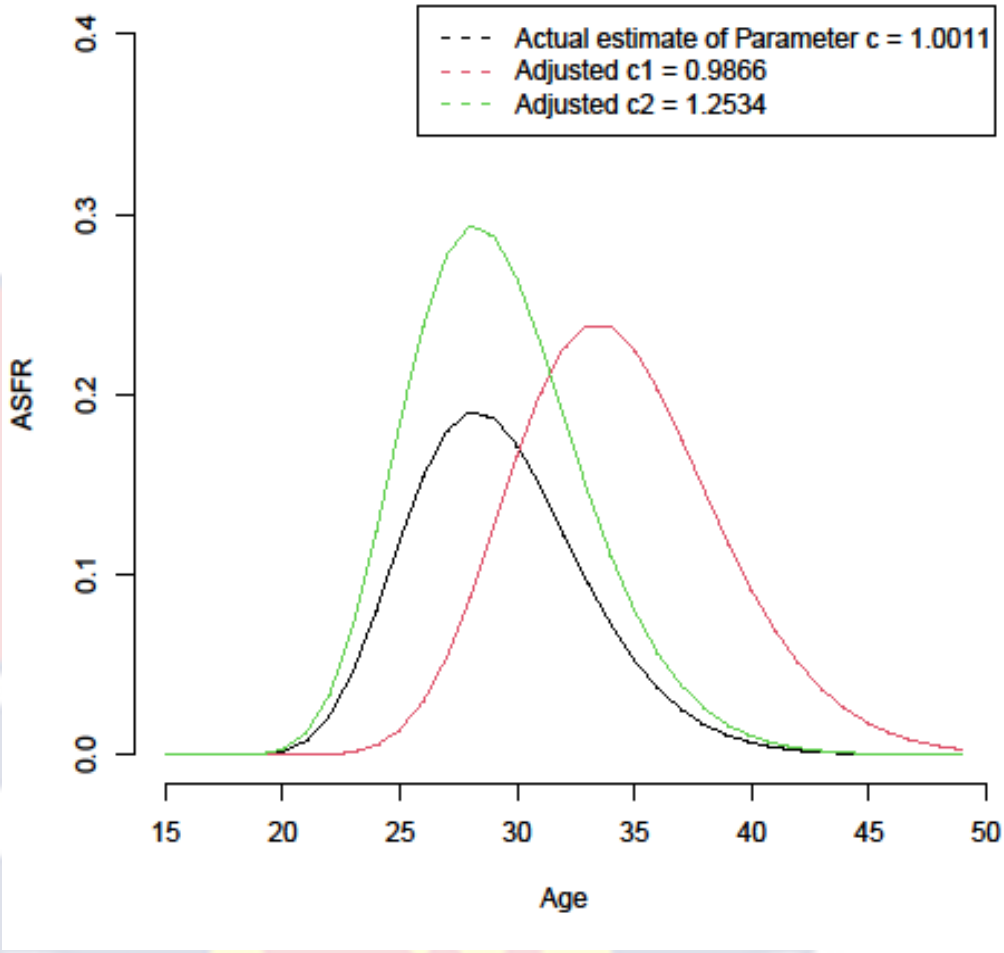

Figure 9: Gamma fertility curves for the parameter *c* at different levels.

Figure 9 shows that when the value of the parameter *c* is high at 1.2534, the ASFR are high and the curve seems to more symmetric across the ages of reproductive period; however, when the value of the parameter *c* falls to 1.0011, the peak of the curve falls short with low ASFR around 0.2 at the age of 29 years and sharply declines to aged 45. It can be noticed that as the value of the parameter continues to fall to 0.9866, the peak of curve rises again and seem to be shifted to right sides, then sharply declines toward age 45 years with broader shape.

The Beta fertility model

The Beta fertility model can be expressed as:

$$f(x) = R\frac{\Gamma(A+B)}{\Gamma(A)\Gamma(B)}(\beta-\alpha)^{-(A+B-1)}(x-\alpha)^{A-1}(\beta-x)^{B-1}$$

for $\alpha < y < \beta$

where, the parameter *R* controls the level of fertility, whereas the parameters α and β indicate the lower and higher age at childbirth, respectively. The parameters A and B are said to be connected to the model's mean, and variance through some relations (Hoem et al. 1981).

Estimation of the parameters of the Beta model

The parameter *R* is related to the total fertility rate of the Beta model and, hence, it is treated as a constant. To estimate the other parameters, the method of maximum likelihood estimation is used.

From Equation (1), the likelihood function of the Beta fertility model is given as

$$L(y) = \left(R\frac{\Gamma(A+B)}{\Gamma(A)\Gamma(B)}\right)^{m}(\beta-\alpha)^{-m(A+B-1)}\prod_{i=0}^{m}(y-\alpha)^{A-1}\prod_{i=0}^{m}(\beta-y)^{B-1}$$

Taking the natural logarithm of the likelihood function gives

$$l(y) = m\ln R + m\ln\Gamma(A+B) - m\ln\Gamma(A) - m\ln\Gamma(B) - m(A+B-1)\ln(\beta-\alpha) + (A-1)\sum_{i=0}^{m}\ln(y-\alpha) + (B-1)\sum_{i=0}^{m}\ln(\beta-y) \quad (14)$$

Taking the partial differential of Equation (14) with respect to *A* and setting the result of the derivative to zero,

$$\frac{\partial l(y)}{\partial A}=\frac{\partial}{\partial A}\left[m\ln\left(R\frac{\Gamma(A+B)}{\Gamma(A)\Gamma(B)}\right)\right]-\frac{\partial}{\partial A}\left(m\ln\Gamma(A)\right)-\frac{\partial}{\partial A}\left[m(A+B-1)\ln(\beta-\alpha)\right]+\frac{\partial}{\partial A}\left[(A-1)\left(\sum_{i=0}^{m}\ln(y-\alpha)\right)\right]=0 \quad (15)$$

From Equation (15), applying the constant multiple rules gives

$$m\frac{\partial}{\partial A}\left\{\ln\Gamma(A+B)\right\}-m\frac{\partial}{\partial A}\left\{\ln\Gamma(A)\right\}-m\ln(\beta-\alpha)\frac{\partial}{\partial A}(A+B-1)+\sum_{i=0}^{m}\ln(y-\alpha)\frac{\partial}{\partial A}(A-1)=0$$

Implies,

$$m\frac{\partial}{\partial A}\left\{\ln\Gamma(A+B)\right\}-m\frac{\partial}{\partial A}\left\{\ln\Gamma(A)\right\}-m\ln(\beta-\alpha)+\sum_{i=0}^{m}\ln(y-\alpha)=0$$

Applying the composite function differentiation technique, the following expression is obtained.

$$m\left[\frac{\partial}{\partial u}\ln(u)\frac{\partial}{\partial A}\Gamma(A+B)\right]-m\left(\frac{\partial}{\partial v}\ln(v)\frac{\partial}{\partial A}\Gamma(A)\right)-m\ln(\beta-\alpha)+\sum_{i=0}^{m}\ln(y-\alpha)=0$$

where, $u=\Gamma(A+B)$ and $v=\Gamma(A)$. That is,

$$m\left(\frac{1}{u}\right)\frac{\partial}{\partial A}\Gamma(A+B)-m\left(\frac{1}{u}\right)\frac{\partial}{\partial A}\Gamma(A)-m\ln(\beta-\alpha)+\sum_{i=0}^{m}\ln(y-\alpha)=0$$

Implies,

$$m\left(\frac{\frac{\partial}{\partial A}\Gamma(A+B)}{\Gamma(A+B)}\right)-m\left(\frac{\frac{\partial}{\partial A}\Gamma(A)}{\Gamma(A)}\right)-m\ln(\beta-\alpha)+\sum_{i=0}^{m}\ln(y-\alpha)=0$$

Equivalently,

$$m\left(\frac{\Gamma\left\{\frac{\partial}{\partial A}(A+B)\right\}}{\Gamma(A+B)}\right)-m\left(\frac{\Gamma\left\{\frac{\partial}{\partial A}(A)\right\}}{\Gamma(A)}\right)-m\ln(\beta-\alpha)+\sum_{i=0}^{m}\ln(y-\alpha)=0$$

Implies,

$$\frac{m}{A+B}-\frac{m}{A}-m\ln(\beta-\alpha)+\sum_{i=0}^{m}\ln(y-\alpha)=0$$

Making B the subject gives

$$B=\frac{m\ln(\beta-\alpha)-\sum_{i=0}^{m}\ln(y-\alpha)}{m} \tag{16}$$

which is the maximum likelihood estimator of B.

Now, taking the partial differential of Equation (14) with respect to the parameter B and setting the result to zero,

$$\frac{\partial l(y)}{\partial B}=\frac{\partial}{\partial B}\left[m\ln\left(R\frac{\Gamma(A+B)}{\Gamma(A)\Gamma(B)}\right)\right]-\frac{\partial}{\partial B}\left(m\ln\Gamma(B)\right)-$$
$$\frac{\partial}{\partial B}\left[m(A+B-1)\ln(\beta-\alpha)\right]+\frac{\partial}{\partial B}\left[(B-1)\left(\sum_{i=0}^{m}\ln(\beta-y)\right)\right]=0$$

That is,

$$m\frac{\partial}{\partial B}\left\{\ln\Gamma(A+B)\right\}-m\frac{\partial}{\partial B}\left\{\ln\Gamma(B)\right\}-m\ln(\beta-\alpha)+$$
$$\frac{\partial}{\partial B}(A+B-1)+\sum_{i=0}^{m}\ln(\beta-y)\frac{\partial}{\partial B}(B-1)=0$$

Applying the composite function differentiation technique,

$$m\left[\frac{\partial}{\partial u}\ln(u)\frac{\partial}{\partial B}\Gamma(A+B)\right]-m\left(\frac{\partial}{\partial u}\ln(u)\frac{\partial}{\partial B}\Gamma(B)\right)$$
$$-m\ln(\beta-\alpha)+\sum_{i=0}^{m}\ln(\beta-y)=0$$

where, $u=\Gamma(A+B)$ and $v=\Gamma(B)$. That is,

$$m\left(\frac{1}{u}\right)\frac{\partial}{\partial B}\Gamma(A+B)-m\left(\frac{1}{u}\right)\frac{\partial}{\partial B}\Gamma(B)-m\ln(\beta-\alpha)+\sum_{i=0}^{m}\ln(\beta-y)=0.$$

Implies,

$$m\left(\frac{\frac{\partial}{\partial B}\Gamma(A+B)}{\Gamma(A+B)}\right)-m\left(\frac{\frac{\partial}{\partial B}\Gamma(B)}{\Gamma(B)}\right)-m\ln(\beta-\alpha)+\sum_{i=0}^{m}\ln(\beta-y)=0,$$

which is equivalent to

$$m\left(\frac{\Gamma\left\{\frac{\partial}{\partial B}(A+B)\right\}}{\Gamma(A+B)}\right)-m\left(\frac{\Gamma\left\{\frac{\partial}{\partial B}(B)\right\}}{\Gamma(B)}\right)-m\ln(\beta-\alpha)+\sum_{i=0}^{m}\ln(\beta-y)=0$$

That is,

$$\frac{m}{A+B}-\frac{m}{B}-m\ln(\beta-\alpha)+\sum_{i=0}^{m}\ln(\beta-y)=0$$

Making A the subject gives

$$A=\frac{m\ln(\beta-\alpha)-\sum_{i=0}^{m}\ln(\beta-y)}{m} \qquad (17)$$

Equation (17) gives the maximum likelihood estimator of the parameter *A*.

Assessing the effect of the parameters of the Beta fertility model

The effects of the parameters, R, A and B, of the Beta fertility model are assessed using the Ghana's ASFR data. A typical Beta fertility curve for the data is presented in Figure 14.

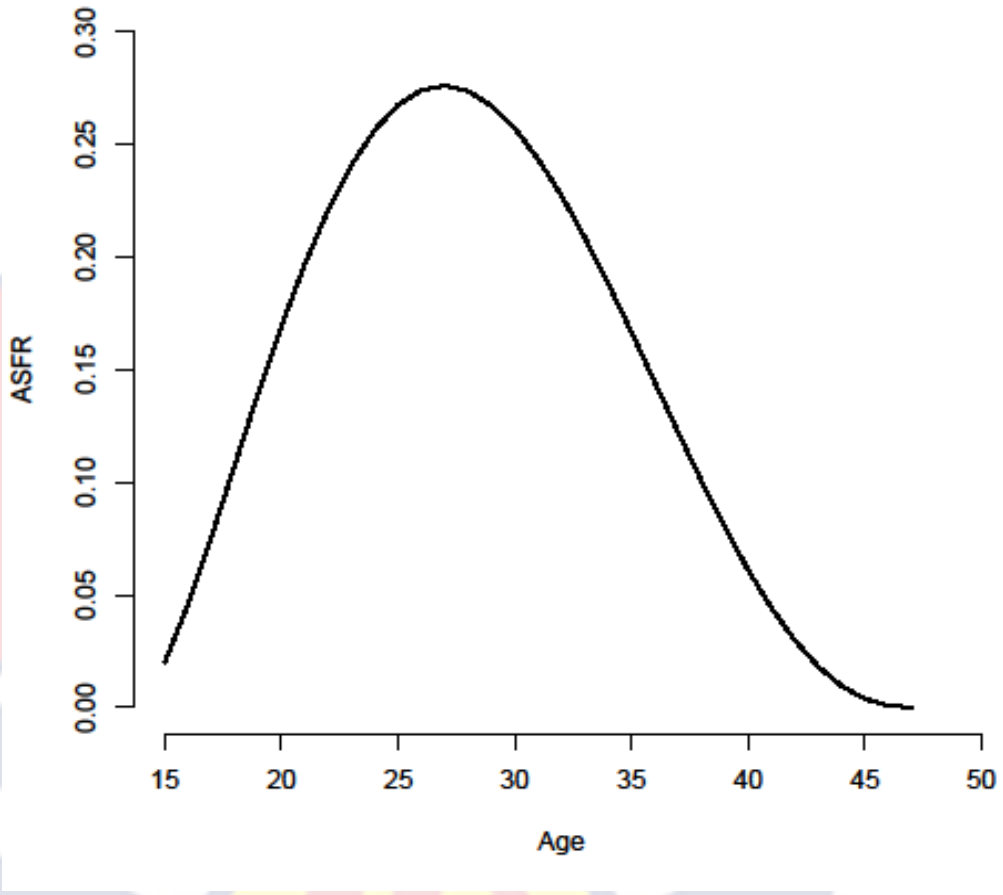

Figure 10: A typical Beta fertility curve using Ghana ASFRs, 2014 – 2020.

The figure shows that the age specific fertility rate rises quickly in the early ages, reaches its peak in the middle ages (25 to 30), and then declines gradually as women get older and stop having children.

Figure 11 displays the results of the assessment of the parameter *R*.

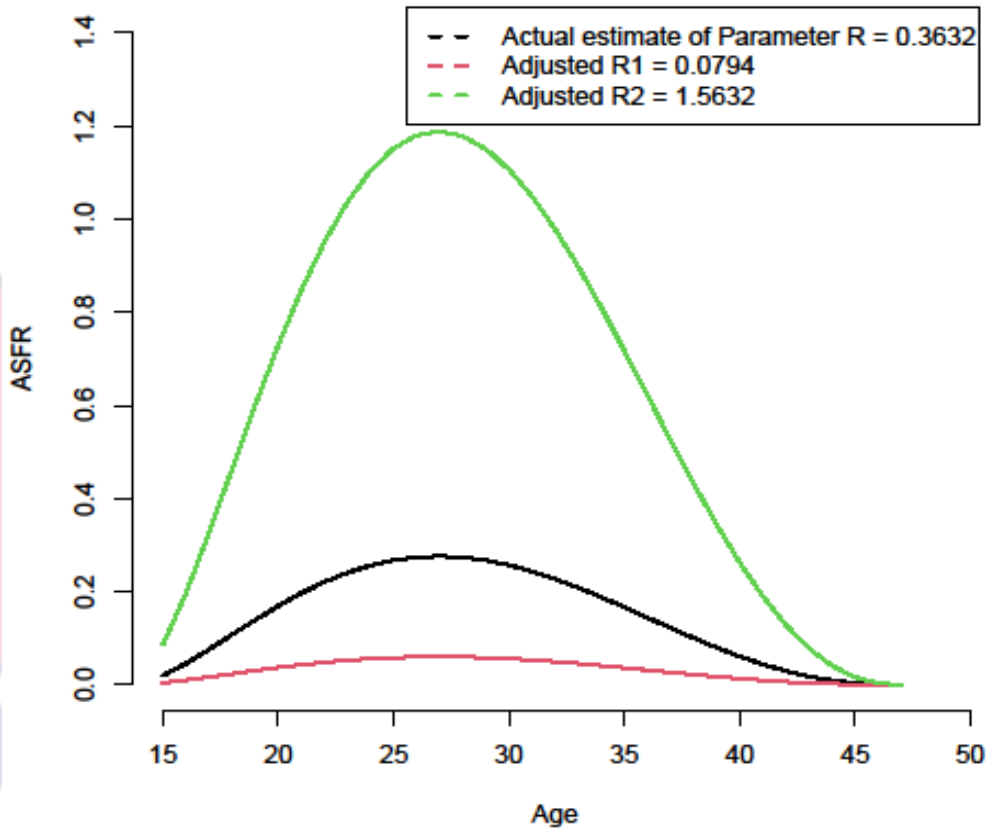

Figure 11: Beta fertility curves for the parameter *R* at different levels.

When the value of the parameter *R* is high at 1.5632, the fertility curve is more symmetric across various ages of the reproductive period. Meanwhile, as the value of the parameter falls to 0.3632, the peak of the curve falls short and flatter out, and the curve becomes linear across the reproduction period when the value of *R* further decreases to 0.0794. Hence, the appropriate shape of the Beta fertility curve is observed when the value of *R* is high.

Figure 12 illustrates different Beta fertility curves for various values of the parameter *A*.

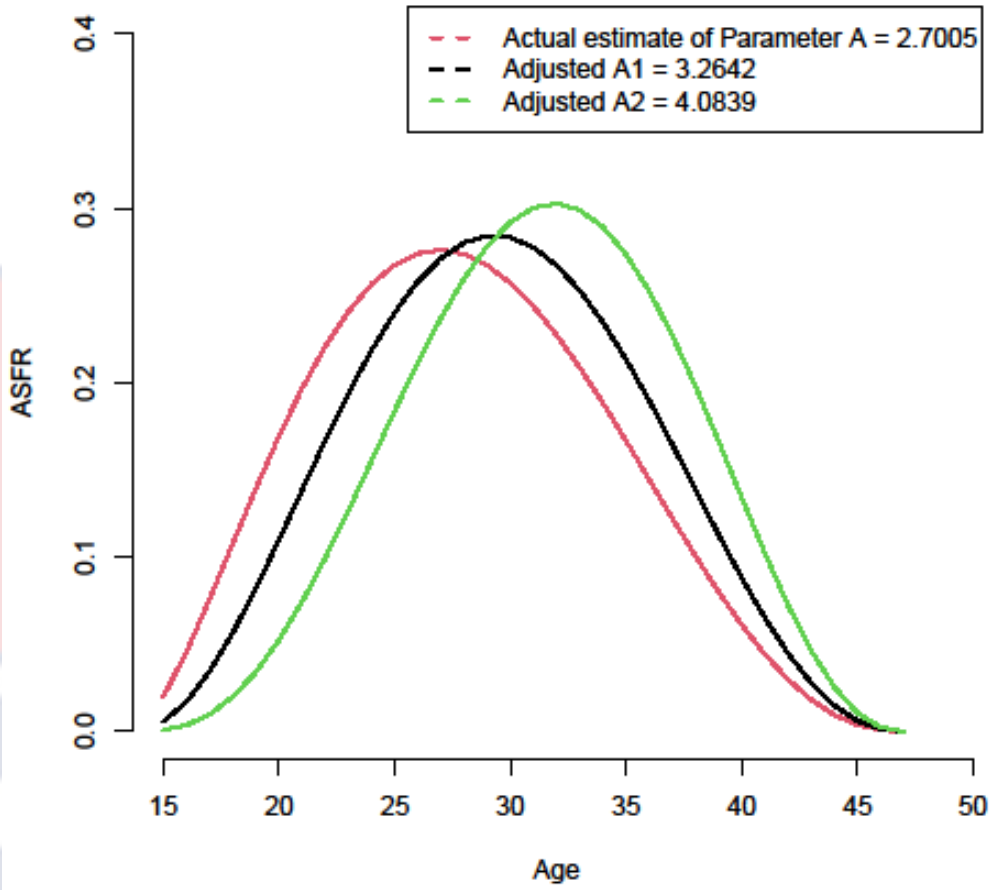

Figure 12: Beta Fertility curves for the parameter *A* at different levels

The results reveal that, for a lowest value of the parameter *A* at 2.7005, the curve skew little to the left side with it peak at age 29 years and fairly board in nature. It can be observed that as the value of the parameter *A* increases, the Beta fertility curves generally shift to the right side with moderately shaped peak. Thus, a high value of *A* depicts a population whose maximum fertility is towards late ages of reproduction.

Figure 13 illustrates different Beta fertility curves for various values of the parameter *B*.

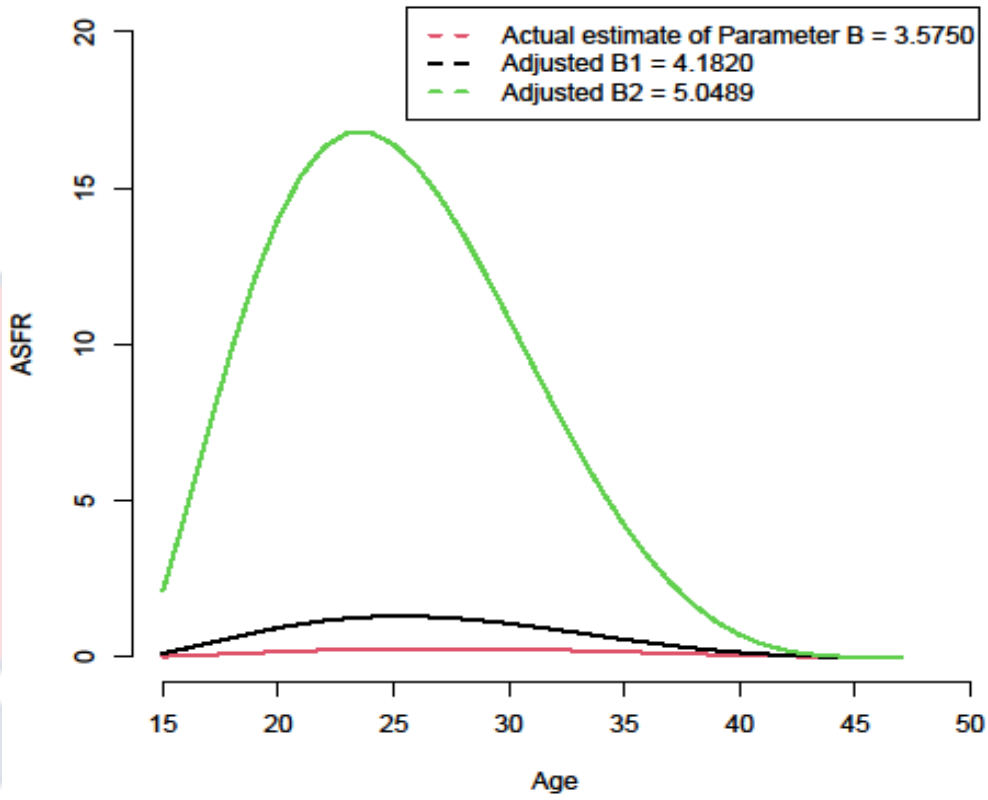

Figure 13: Beta fertility curves for the parameter *B* at different levels

When the value of the parameter *B* is high at 5.0489, the shape of the Beta fertility curve is conspicuous and more definitive. However, when the value of b decreases, the shape of the Beta fertility curve generally deteriorates across the reproduction period. Therefore, a high value of *B* is required to completely characterized the fertility of a given population.

The Concept of Time Series Analysis

A time series is a sequence of observations that changes over time, denoted by X_t, where t is an integer that stands for the time steps. The observations may be taken every hour, day, week, month, or year, or at any other regular interval. Although the ordering is usually through time, particularly in terms of some equally spaced time intervals, the ordering may also be taken

through other dimensions, such as age. Time series occur in a variety of fields, for example, annual birth rates, and mortality rates. The list of areas in which time series is observed and studied is endless.

Various time series models have been employed in several studies (e.g., Deb & Chakrabarty, 2016; McNown & Rajbhandary, 2003; Thompson, Bell, Long & Miller, 1989) to forecast fertility rates. This study attempts to determine an appropriate time series model to forecast Ghana's fertility rate.

General patterns of a time series

Trend and seasonality are the two main kinds of components used to explain time series patterns. The series depicts a broad, systematic linear or nonlinear element of the trend that evolves over time but does not replicate within the time window covered by the data. On the seasonal part, however, the sequence consistently repeats itself over time at regular intervals. These two broad categories of time series elements might coexist in actual data. Cyclical and irregular patterns are two other patterns that can be observed in time series analysis.

Trend analysis

There seems to be no "automatic" methods that have been demonstrated to reliably detect trend mechanisms in time series data. Yet, that portion of the data analysis is often not too challenging provided the pattern is monotonous (continuously increasing or decreasing). Smoothing is the initial step on the path of trend discovery if indeed the data have a significant amount of error.

Seasonality analysis

Another element of time series pattern that is generally present is seasonal dependence (seasonality). Formally speaking, it is described by way of correlation dependency of order g between each i^{th} component in the series and the $(i-g)^{th}$ component, restrained by autocorrelation (that is, a connection among the two terms); g is typically referred to as the lag. If indeed the measurement error is not too large, the patterns that recurrences every g elements in the series can be used to visually identify seasonality.

Stationarity and Non-stationarity of Time Series

The properties of a random process – such as the mean, variance, autocorrelation, and n^{th} order distribution – are examples of the conditions for stationarity, because they are all be time invariant. In order for a random process W_n to be considered strictly stable, all of its finite order distributions must be time invariant, which means that the joint cumulative distribution function (CDFs) (probability density functions [pdfs], probability mass functions [pmfs]) of $W(t_1), W(t_2), \cdots, W(t_g)$ and $W(t_{1+\tau}), W(t_{2+\tau}), \cdots, W(t_{g+\tau})$ are same for g, for all $t_1, t_2, \cdots, t_g$ and all-time shifts τ. A time series is referred as non-stationary if it is not stationary. The following is an easy non-stationary time series model:

$$W(t) = \mu_t + \varepsilon_t$$

where ε_t is a weakly stationary series and the mean (μ_t) is a function of time. The stationary condition guarantees that the moving average and autoregressive variables in the hypothesized model are invertible and stable within a given

range. Consequently, the approximated model might be utilized to forecast if such condition is secured (Hamilton, 1994).

Autocorrelation Function

The general procedure used to create a forecasting model is very well described by the autocorrelation function (ACF). It assesses how closely adjacent observations in a time series are correlated. The autocorrelation function at any lag g, ρ_g is defined as

$$\rho_g = \frac{\operatorname{cov}\left(X_t, X_{t-g}\right)}{\delta_{X_t}\delta_{X_{t-g}}} = \frac{\mathrm{E}\left[\left(X_t - \mu_\gamma\right)\left(X_{t-g} - \mu_\gamma\right)\right]}{\mathrm{E}\left[\left(X_t - \mu_\gamma\right)^2\left(X_{t-g} - \mu_\gamma\right)^2\right]}$$

where X_t, X_{t-g}, and μ_t represent the observation at time t, time $t-g$, and the observed mean, respectively. Although theoretically autocorrelation function is typically unknown, the sample autocorrelation function ρ_g can be used to make estimates for ρ_g. That is,

$$\hat{\rho}_g = \frac{\sum_{t=1}^{m}\left(X_t - \overline{X}\right)\left(X_{t-g} - \overline{X}\right)}{\sum_{t=1}^{m}\left(X_t - \overline{X}\right)^2}$$

where t is the time series' length, X is the observation's mean, and $g = 1, 2, \ldots$. If X_t and X_{t-g} define the covariance between them as γ_g then,

$$\rho_g = \frac{\gamma_g}{\gamma_0}$$

Thus, for any stochastic process $\rho_0 = 1$, it is likewise true that $\rho_g = \rho_{-g}$

Partial Autocorrelation Function

Once the impacts of all other time lags are held constant, the partial autocorrelation coefficient (PACF) estimates the degree of relationship between an observation X_t and X_{t-k}. When we are unsure of the proper order for autoregressive process to match the time series, we take partial autocorrelation into account. The term used to signify and characterize PACF is

$$Q_{kk} = \frac{\left|P_k^*\right|}{\left|P_k\right|}$$

where P_k^* is a P_k with the least column replaced by $\left[\rho_1, \rho_2, ..., \rho_k\right]^{\mathrm{T}}$ and P_k is a $k \times k$ autocorrelation matrix.

Regressing X_t on $X_{t-1}, X_{t-2}, \ldots, X_{t-k}$ yields the partial autocorrelation coefficient of order k, denoted by the symbol α_k. That is,

$$X_t = \beta_0 + \beta_1 X_{t-1} + \beta_2 X_{t-2} + ... + \beta_k X_{t-k}$$

The forecast variable X_t's historical values serve as the explanatory variables $\left(X_{t-i}\right)$, while the estimated coefficient β_k from the regression equation above serves as the partial autocorrelation $\left(\alpha_k\right)$.

The General Autoregressive Model

The foundation of autoregressive models is the notion that the present value of a sequence, W_t, may be understood as a function of p earlier values, $W_{t-1}, W_{t-2}, \ldots, W_{t-p}$ where g specifies the number of steps into the past that must be forecasted in order to predict the present value. The formula for autoregressive model of order p, denoted by $AR(p)$, is

$$W_t = \alpha + \theta_1 W_{t-1} + \theta_2 W_{t-2} + ... + \theta_p W_{t-p} + \varepsilon_t$$

where, $\theta_1, \theta_2, \cdots, \theta_p$ are the parameters of the $AR(p)$ model. We presume that the series ε_t is a Gaussian white noise with mean zero (0) and variance σ_ε^2 unless otherwise specified.

The Moving Average Model

The moving average model of order q denoted by $MA(q)$ is defined as

$$W_t = \varepsilon_t + \phi_1 \varepsilon_{t-1} + \phi_2 \varepsilon_{t-2} + \cdots + \phi_q \varepsilon_{t-q}$$

where $\phi_1, \phi_2, \cdots, \phi_q \ (\phi_q \neq 0)$ are parameters of the model. It is assumed that ε_t noise.

Autoregressive Integrated Moving Average Model

The term "Autoregressive Integrated Moving Average" is abbreviated as "ARIMA". A time series that needs to be differenced in order to achieve stationarity is referred to as a "integrated" version of the stationary series. Lags of the differenced series that appear in the forecasting equation are referred to as "Autoregressive" terms, while lags of the forecast errors are referred to as "Moving Average" terms.

In an "$ARIMA(p,d,q)$" structure, p is the number of Autoregressive elements, d is the degree of differencing, and q is the degree of lagged prediction errors (Moving Average) in the prediction equation.

If $\nabla^d W_t = (1 - B_a)^q W_t$ is stationary $ARMA(p,q)$, then a process W_t is said to be $ARIMA(p,d,q)$. In other words, after differencing a non-seasonal

process d time, the process ought to be stationary. The model is typically expressed as

$$\phi(B_a)(1-B_a)^d W_t = \theta(B_a)\varepsilon_t$$

If $\mathrm{E}(\nabla^d W_t) = \mu_a$, then the model should be written as:

$$\phi(B_a)(1-B_a)^d W_t = \alpha_a + \theta(B_a)\varepsilon_t$$

where $\alpha_a = (1-\phi_1 - \cdots - \phi_p)$.

Seasonal Autoregressive Integrated Moving Average Model

The famous Box-Jenkins ARIMA model has been generalized as the Seasonal Autoregressive Integrated Moving Average (SARIMA) model to accept data with both seasonal and non-seasonal features. When the series includes both seasonal and non-seasonal behaviors, the ARIMA model generalizes to SARIMA model. The ARIMA model is ineffective when applied to the series because of this characteristic of the series.

The Multiplicative Seasonal Autoregressive Integrated Moving Average model, or SARIMA for short, is also known as the $ARIMA(p,d,q)(P,D,Q)S$ model. In its lag version, this could be expressed as follows (Halim & Bisono, 2008):

$$\varphi(L_a)\gamma(L_a^s)(1-L_a)^d(1-L_a^s)^D y_t = \phi(L_a)\varpi(L_a^s)\varepsilon_t$$

where,

$$\varphi(L_a) = 1-\varphi_1 L_a - \varphi_2 L_a^2 - \cdots - \varphi_p L_a^p,$$

$$\gamma(L_a^s) = 1-\gamma_1 L_a^S - \gamma_2 L_a^{2S} - \cdots - \gamma_p L_a^{PS},$$

$$\phi(L_a) = 1+\phi_1 L_a + \phi_2 L_a^2 + \cdots + \phi_q L_a^q,$$

and

$$\varpi\left(L_a^{\,s}\right)=1-\varpi_1 L_a^{\,S}-\varpi_2 L_a^{\,2S}-\cdots-\varpi_q L_a^{\,QS}.$$

The non-seasonal AR, differencing, and MA orders are represented by p, d, and q, respectively, while the seasonal AR, Differencing, and MA orders are represented by P, D, and Q. Y_t is for observable time series data at period t, ε_t stands for white noise (random shock) at period t, L_a for backward shift operator, and S for seasonal order. The sample autocorrelations and partial autocorrelation functions are assessed to identify the suitable model based on the amount of nonseasonal and seasonal differences needed to make the time series stable (Apergis, Mervar & Payne, 2017).

Model Performance Measure

It is vital to check the performance of the various model employed in the study while modeling the ASFR. Typically, the projected and observed ASFR values from a model are shown, and the best fit among all the models is chosen.

Sum of square error

The Sum of squares error (SSE) should be determined for each model in quantitative terms, the model with the lowest SSE being the best fit model. As a result, the sum of squares owed to error (SSE) for the model parameters has been minimized. The SSE function can mathematically be expressed as

$$SSE=\sum_s\left[f\left(y\right)-f\left(\hat{y}\right)\right]^2$$

where $f(\hat{y})$ is the predicted ASFR at age y from the different models employed in this study and $f(y)$ stands for the experimental ASFR at age y.

Akaike's information criteria and corrected Akaike's information criteria

Checking the effectiveness of various models is crucial while modeling the ASFR. SSE ought to be calculated for each model, and the one with the lowest SSE is the best fit model. However, the SSE will not solve the heightened model complexity brought on by the addition of extra parameters. To maintain the model's fitness and account for the complexity, we applied Akaike's Information Criteria (AIC) and the Corrected Akaike's information Criteria (AICc).

The Akaike's Information Criteria are modified in the corrected Akaike's Information Criteria (AICc) to account for limited sample sizes. The SSE is adjusted by the AIC for a certain model liable on the quantity of variables and observations in the data. The AIC can be expressed mathematically as

$$AIC = 2w + m\ln\left(\frac{SSE}{m-w}\right).$$

Similarly, the AICc can be expressed as

$$AICc = AIC + \frac{2w(w+1)}{(m-w-1)}$$

where, w signifies the number of parameters existing in a model, m represents the number of observations, and SSE denotes sum of squares error.

Description of Dataset Used for the Study

The data used for the study were sourced from national headquarters of the Ghana Health Service, Accra. The dataset spans the years 2014 – 2020 and is made up of number of live births for women in the reproductive period. The dataset also includes the age of the mother at the time of delivery. Another variable in the dataset is the mid-year population of females in Ghana who are in the fecundity period.

In order to forecast fertility rates of Ghana for the period 2021 – 2023, estimates of age specific fertility rates (ASFRs) ($\hat{y}_{t-(t+5)}$) are obtained based the selected fertility model. These estimates of ASFRs are used as input for time series analysis of the fertility of Ghana. The structure of the data for time series analysis is presented in Table 1.

Table 1: Data Structure for Time Series Analysis

Year	Age Group	Group No.	Estimate of ASFR
2014	15 – 19	1	$\hat{y}_{15-19}$
	20 – 24	2	$\hat{y}_{20-24}$
	25 – 29	3	$\hat{y}_{25-29}$
	30 – 34	4	$\hat{y}_{30-34}$
	35 – 39	5	$\hat{y}_{35-39}$
	40 – 44	6	$\hat{y}_{40-44}$
	45 – 49	7	$\hat{y}_{45-49}$
2015	15 – 19	1	$\hat{y}_{15-19}$
	⋮	⋮	⋮
	45 – 49	7	$\hat{y}_{45-49}$
⋮	⋮	⋮	⋮
2020	15 – 19	1	$\hat{y}_{15-19}$
	⋮	⋮	⋮
	45 – 49	7	$\hat{y}_{45-49}$

Source: Researcher's own computation, (2022)

Data Analyses Procedure

The analyses of data used for the study were largely based on age specific fertility rates (ASFRs), which is a fertility indicator. In view of this, ASFRs were computed in Microsoft Excel 2019. In this study, the fertility of Ghana for the period under consideration is explored using descriptive statistics such as the mean, standard deviation, minimum and maximum values, and skewness. The results of the analyses have been presented in the form of tables and graphs.

Further analyses of the data were conducted using some standard fertility models and time series analysis technique. The implementation of the methods employed in this study with application to the Ghana fertility dataset were done using the *R* statistical software. The various fertility models' fitting and estimation were performed using the *fmsb* package in *R* (Nakazawa, 2018). Additionally, the performance assessment of the fertility models was based on the *SSE*, *AIC* and *CAIC* (Hurvich & Tsai, 1989; Akaike, 1974). Finally, a univariate time series was employed and implement to predict fertility of Ghana for the period 2021 to 2023, using the *forecast* and *fpp2* packages in *R* (Hyndman & Khandakar, 2008; Hyndman & Athanasopoulos, 2018).

Chapter Summary

The chapter reviewed some standard age specific fertility rate models, and mean age at childbearing. The assessment of the behaviors of the various parameters of the models are presented in the chapter. It looks at the general patterns of time series analysis such as trend and seasonality, the autocorrelation function (ACF), partial autocorrelation function (PACF), the autoregressive integrated moving average (ARIMA) and seasonal autoregressive integrated moving average (SARIMA).

CHAPTER FOUR

RESULTS AND DISCUSSION

Introduction

The main objective of the study is to determine the model that best fits Ghana's fertility data. In this regard, three standard fertility models – Hadwiger, Gamma, and Beta – are examined in order to select the model that optimally fits the fertility rate of Ghana. Fertility estimates from the best model selected is further employed in Time Series Analysis for purposes of forecasting Ghana's fertility rate. The chapter presents the results of analyses of the fertility of Ghana in tandem with the objectives of the study. In what follows, the study explores Ghana's fertility data using summary statistics and age specific fertility rate.

Exploring Ghana's Fertility Data for the period 2014 – 2020

The section presents the results of preliminary analysis of Ghana's fertility data using summary statistics such as the minimum and maximum values, the mean, the standard deviation, and the coefficient of skewness. The section also presents the summary of age specific fertility rates (ASFRs) for the dataset. The ASFRs are also represented graphically to discover the fertility structure of Ghana. Table 1 shows the summary statistics for Ghana's fertility data.

Table 2: Summary Statistics for Ghana's Fertility, 2014 – 2020.

Variable	Mean	SD	Min.	Max.	Skewness
Age	32	10.24695	15	49	0
ASFR2014	7.30E-04	5.46E-04	5.66E-06	1.56E-03	8.20E-02
ASFR2015	5.40E-04	4.10E-04	2.93E-06	1.34E-03	1.93E-01
ASFR2016	4.42E-04	3.32E-04	3.07E-06	1.02E-03	1.19E-01
ASFR2017	4.06E-04	2.95E-04	3.07E-06	8.93E-04	2.96E-02
ASFR2018	3.85E-04	2.76E-04	4.04E-06	8.28E-04	4.38E-04
ASFR2019	4.25E-04	3.06E-04	3.08E-06	9.32E-04	9.31E-04
ASFR2020	3.90E-04	2.77E-04	4.30E-06	8.81E-04	-1.49E-02
ASFR2014-2020	3.32E-03	2.41E-03	4.07E-05	7.41E-03	2.94E-02

Source: Researcher's own computation, (2022)

The results show that the mean age of women at childbearing is 32 years with a standard deviation of 10.24695. Again, the ages of women at childbearing lingers between 15 and 49 years, which are normally distributed. In the year 2014, there were 73 live births per 100,000 women from each reproductive age group. The number of live births lingered between about 57 per 1,000,000 and 156 per 100,000 women. The number of births across various age groups was fairly positively skewed, indicating that the number of live deliveries from most age groups was a little less than the average of 73 per 100,000 women. All the years, except 2020, had ASFRs being moderately positively skewed.

For the period under study, the year 2014 had the highest mean number of births (73) per 100,000 women, which decreased on yearly basis, with the year 2018 recording the lowest mean value (about 39). In the year 2018, the number of live births ranged between about 28 and 83 per 100,000 women.

Overall, there were 332 live births per 100,000 women across all age groups for the period 2014 – 2020. In the period, number of live births lingered between about 41 per 1,000,000 and 741 per 100,000 women.

Figure 14 *A* and *B* depicts the observed age-specific fertility rate of Ghana from the year 2014 to 2020.

Figure 14 depicts the observed age-specific fertility rate of Ghana from the year 2014 to 2020.

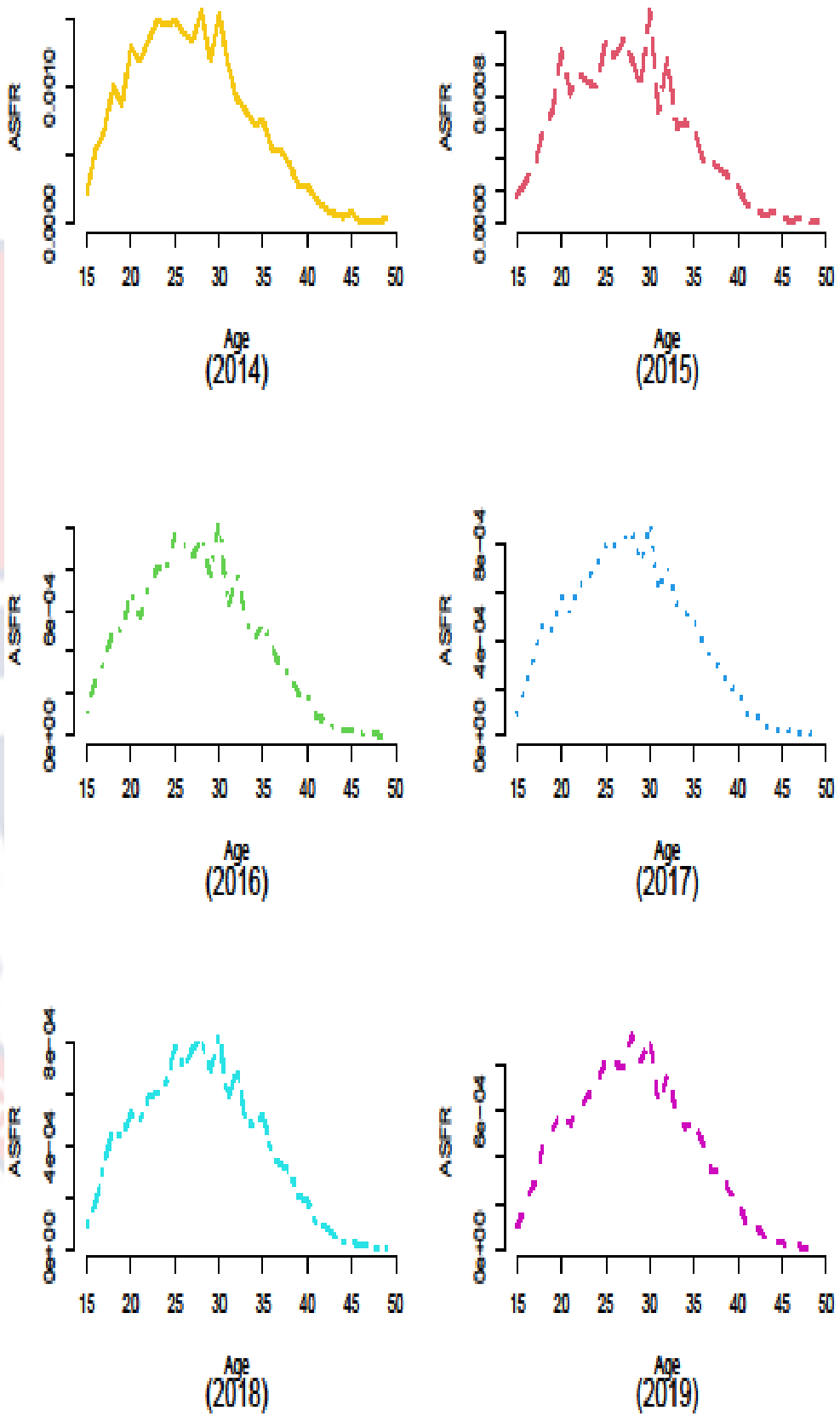

Figure 14: Plot of actual age-specific fertility rate for the years of Ghana from 2014 to 2020

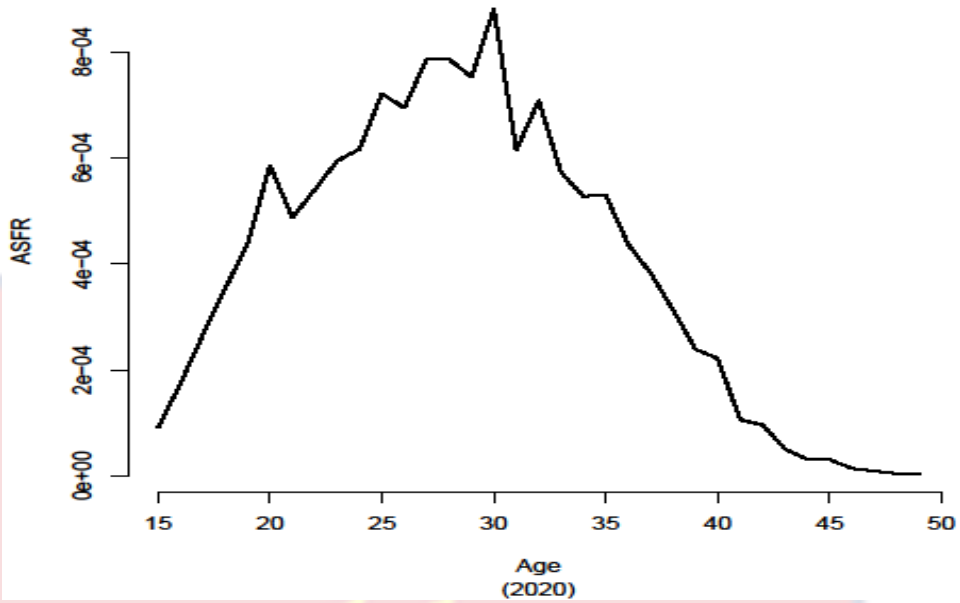

Figure 14 continued

The results show that, in the year 2014, fertility was low at the age of 15; thereafter, it increased and reaches its peak among women in the 25 – 30 age group, subsequently starts to decrease and became low for women in 40 – 49 age category. However, the delay in giving birth is seen in the year 2015 and the others years under consideration. In addition, most of the births occur at age 20 to 33, hence the number of young mothers (ages 15 to 19) decreases. It can be observed that fertility among young mothers (aged 15 to 20) falls sharply in the year 2016, but increased for mothers aged 30 to 35.

In addition, there was a sharp rise in the fertility rate for mothers at age 15 to 20, and then slightly vary for the mothers at age 20 to 32, and a sharp decline from age 33 to 49 in the year 2017. The peak of the fertility curve occurred in the age group 25 to 30 for the year 2017. In the year 2018, there were slightly steady variations between the age group 20 to 35 with the peak of the curve at the age group 25 to 30. The number of births among young mothers continues to decline, leading the curve to start almost at zero.

The results show that, in the year 2019, the fertility rate was mostly recorded in the age group 20 to 35, with the maximum fertility rate for women in ages 25 to 30 category. However, there were little variations throughout the period. There were rapid variations within the year 2020. Women at age 30 recorded the highest number of deliveries. There was a slightly steady decline in ASFR recorded from the age of 33 to the end of the period under investigation.

Figure 15 compares observed ASFRs for various years in the period.

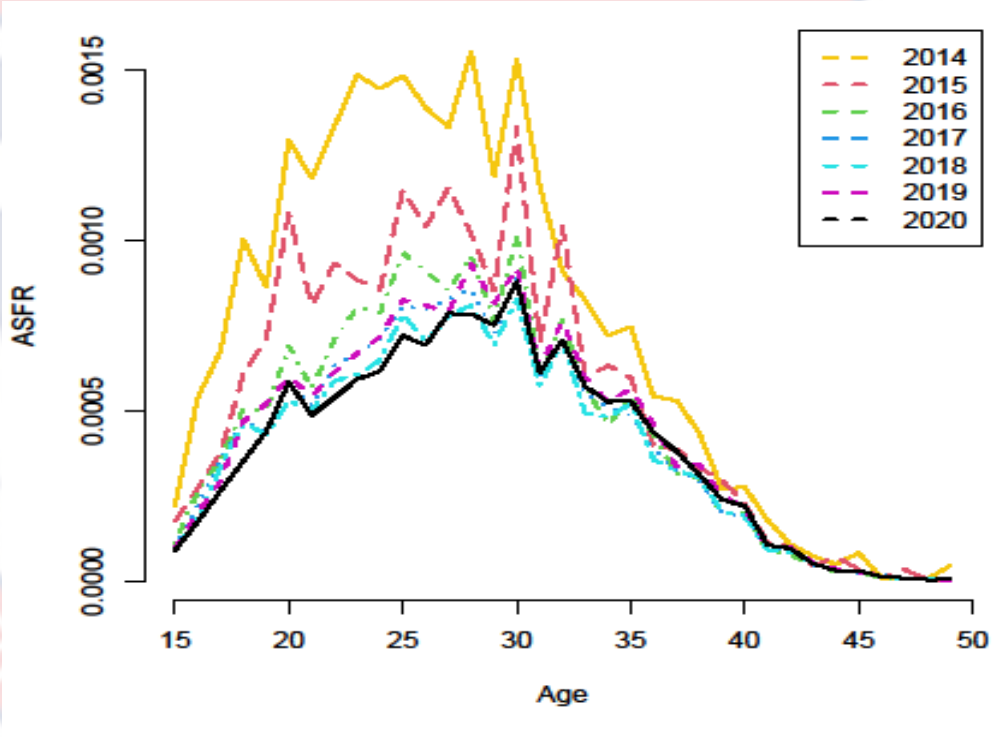

Figure 15: Comparing yearly actual age-specific fertility rate of Ghana from 2014 to 2020.

The results show that, there were abrupt variations in the age-specific fertility rate (ASFR) throughout the various years under study. This pattern is similar to the remaining years with a few alterations in magnitude. The ASFR

rises quickly in the early years, peaks in the middle ages (25 to 30), and then plummets as the reproductive time progresses. At various ages, the selected years have varying amounts of fertility, resulting in variation of total fertility rate.

Also, the highest fertility rate was in 2014, followed by 2015, 2016, 2019, 2017, 2018, and 2020. The value of the peak fertility and the age at which it is reached fluctuate throughout time. In the later ages of reproduction (35 to 49), the year 2014 had the highest level of fertility, while the year 2018 had the lowest level of fertility. The delay in giving birth can be seen in the year 2015. The number of births for young women (mothers) aged 20 to 25 is rapidly declining, while the number of births for mothers aged 26 to 35 is also declining.

In addition, the number of births in the age range 15 to 20 continues to decline for the years under investigation. The highest ASFR was recorded at the age of 30 for all the years except the year 2014 which had its highest ASFR at the age of 25. This indicates that most women in Ghana had their children at the early part of their reproductive age (20 to 25) from 2014 to 2015. There was a delay in giving birth within the country, which led to the mean age of women at birth to shift to age 30 for the period 2015 through to 2020.

Figure 16 shows the actual ASFR for the entire period, 2014 – 2020.

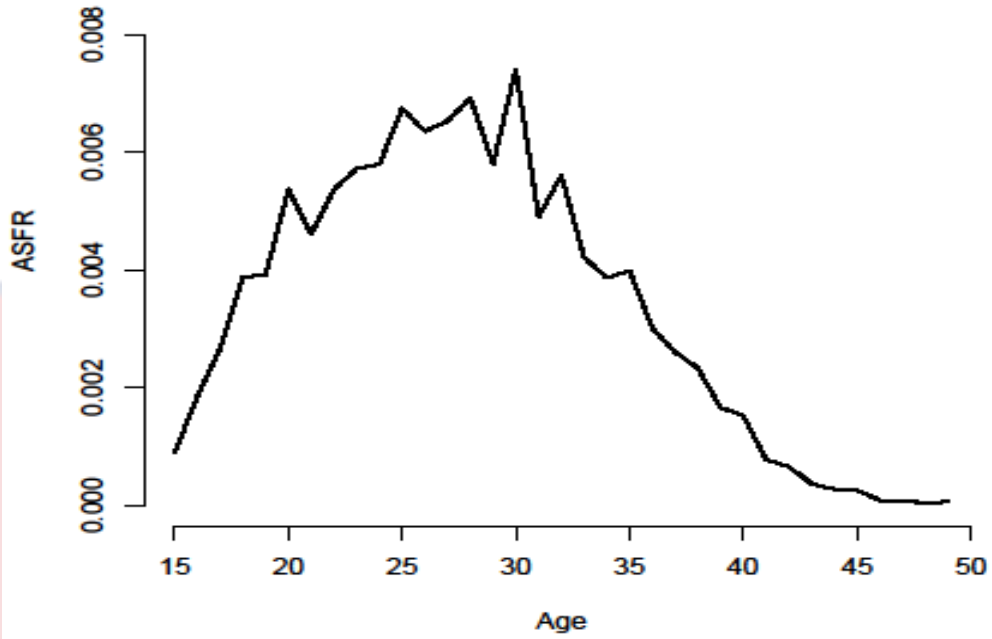

Figure 16: Plot of ASFR of Ghana for the period 2014 – 2020.

It is clear from Figure 16 that, fertility increased slowly from age 15, then varies from age 20 until it reached its peaks for women at age 30, and it declined sharply for women at age 33 and rose a little, then it continued to decline to zero for women at age 50.

However, it is seen in the aggregated age-specific fertility rate that most of the women in the country had their children around the ages of 20 to 35 years.

Fitting Fertility Models to Ghana's Data

The section presents the results of fitting three standard fertility models to Ghana's data. When fitting models to data, an indispensable step is to estimate parameters of the given model. To this end, the parameters of the standard fertility models have been estimated using Ghana's data (see Appendix A). In what follows, a presentation is done on fitting the Hadwiger model to the fertility data of Ghana.

Assessing the Hadwiger model on Ghana's fertility data

Here, an assessment of the Hadwiger model on the observed ASFR of Ghana's is presented. The model is fitted to the observed ASFR for each year to determine how closely it mimics the observed ASFR for Ghana. Figure 17 *A* and *B* shows the fitted Hadwiger model to the observed ASFR for various years under study.

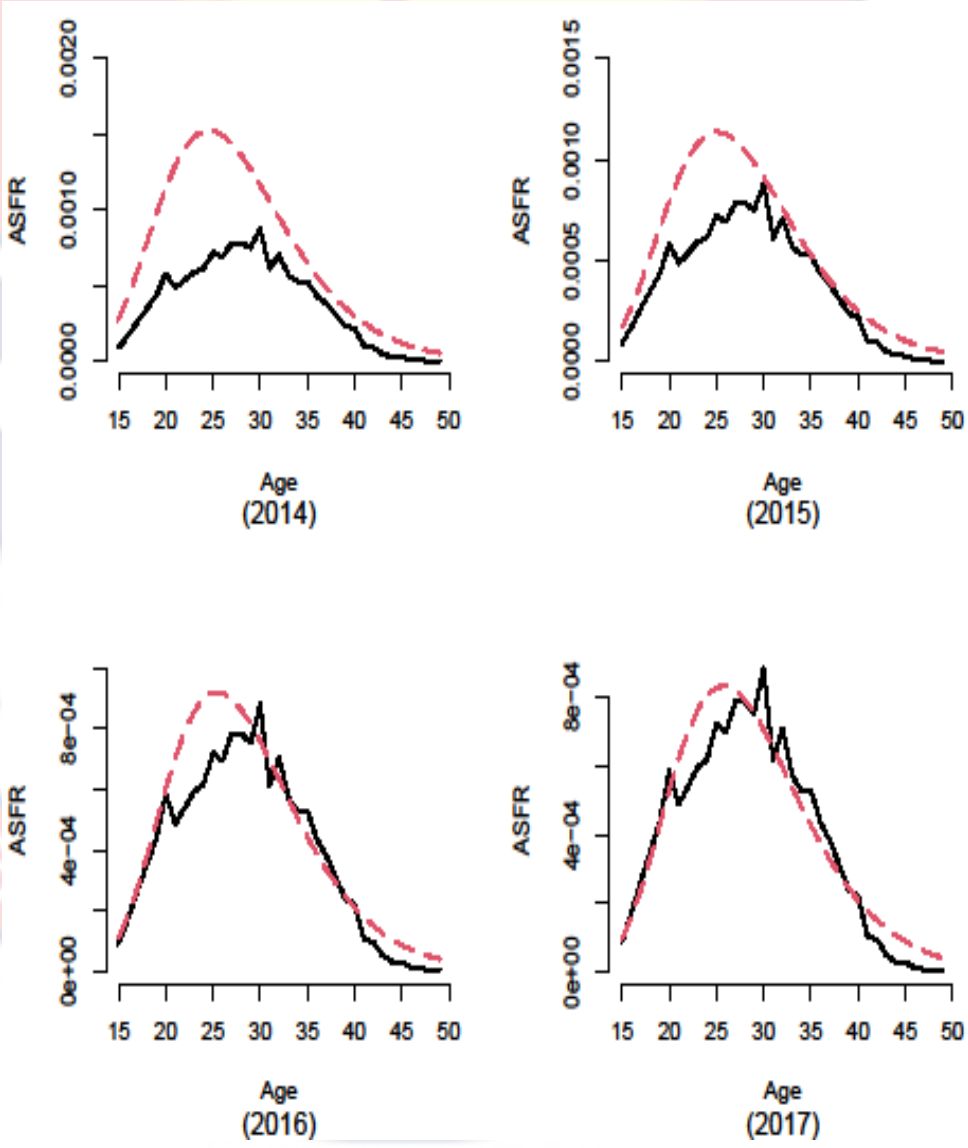

Figure 17 A: Hadwiger fertility model's curves and actual ASFR for the years 2014 to 2017 of Ghana

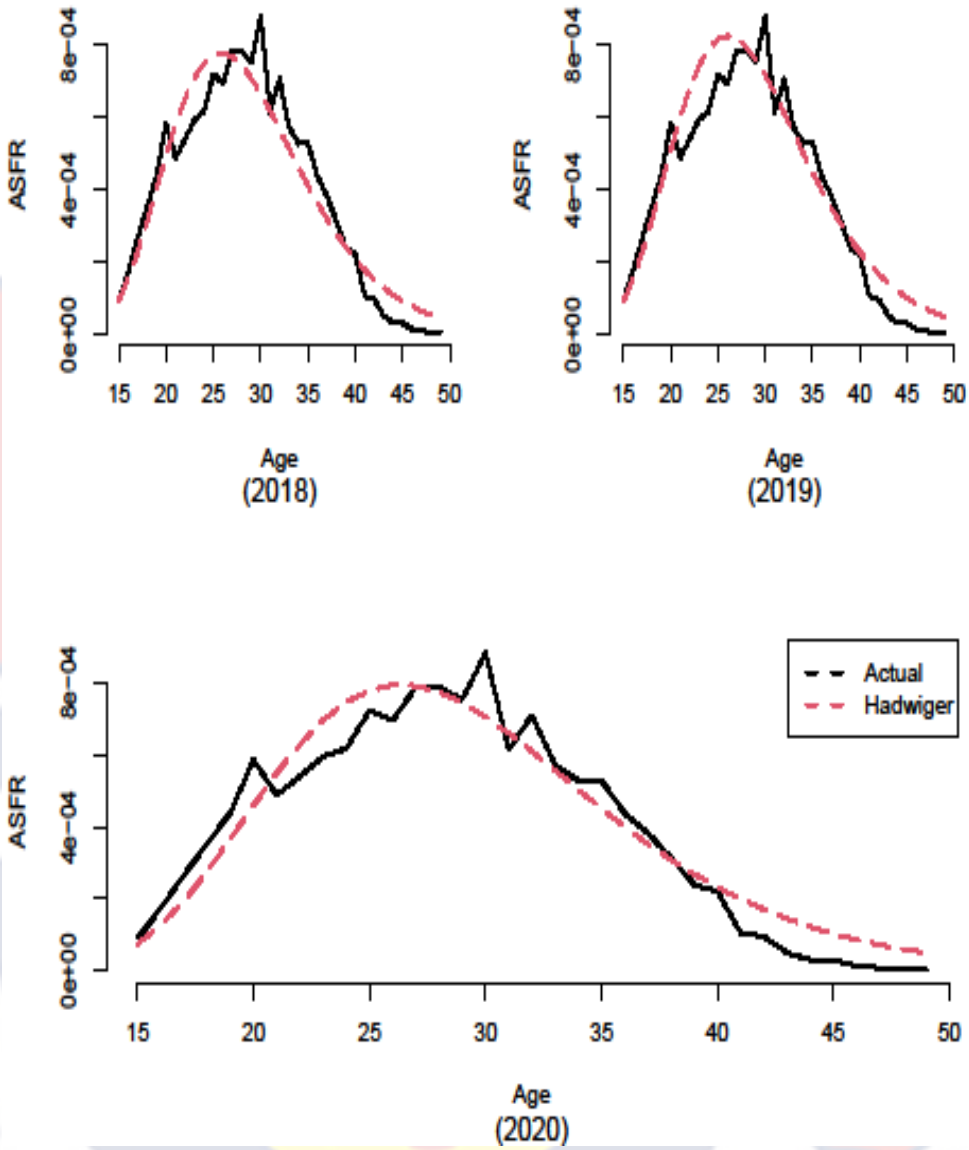

Figure 17 B: Hadwiger fertility model's curves and actual ASFR for the years 2018 to 2020 of Ghana

The results show that the distribution of Ghana's fertility data is somewhat positively skewed. The result conforms to Vahi (2017), who noted that asymmetrical bell-shaped fertility curve is a characteristic of the fertility curves of several European countries. The Hadwiger model closely follows the underlying distribution of the fertility of Ghana. However, in some few instances the Hadwiger model fairly overestimates the fertility of Ghana, notably the years 2016, 2015 and 2014. There is maximum overestimation of

fertility in the year 2014. Typically, fertility peak a bit early for the Hadwiger model than the observed ASFR. In this case, fertility is highest among women at age 25 for the Hadwiger model compared to the age of 30 for the observed ASFR. In a broader perspective, it can be seen that in most of the years, fertility peaked among women in the 25 – 30 age category. This observation particularly holds for both the Hadwiger model and the observed ASFR.

Specifically, the results show that, in the years 2020 and 2019, the Hadwiger fertility curve is much similar to that of the actual ASFR, but still overestimated the ASFR from the ages 20 to 30 years. The model accurately estimates the ASFR for the ages of 30 to 40 years, and slightly rises for ages 40 to 49 years. The figure 17 *A* and *B* clearly shows that the Hadwiger model fits the fertility data more accurately in the year 2018 and 2015, except for the age groups of 20 – 30 and 40 – 49.

Also, in the year 2017, the Hadwiger model accurately estimates the values of ASFR for the early ages (15 to 20) but overestimates for the ages of 21 to 29 and 41 to 49. While it underestimated the values of ASFR for ages 26 to 33. Also, in the years 2014 and 2016, the Hadwiger model estimates the values of the ASFR for the early ages (15 to 20), accurately estimated the values of ASFR for ages 31 to 40 in the year 2014 but underestimated the values of the ASFR for ages 26 to 34 for the year 2016. Whereas, there is an overestimation of the values of ASFR for the ages of 41 to 49 for both 2016 and 2014.

Fitting the Gamma and Beta models to Ghana's fertility data

The study investigates the fitness of the Gamma and Beta models to the actual ASFRs for various years under consideration. The results are presented graphically in Appendix B.

It is worthy of note that the Gamma model does not follow the distribution of the fertility of Ghana. The results show that the Gamma model underestimated the values of the ASFRs for almost all women in reproductive ages, 15 to 44, but slightly accurately estimated the values of the ASFRs for ages 46 to 49.

In addition, an assessment is done on the fitness of the Beta model to the fertility of Ghana (see Appendix B) shows that the curve for the Beta model is conspicuously not similar to the distribution of Ghana's fertility. The results indicate that the Beta model underestimates the values of the ASFRs for all reproductive ages between 15 and 44 years, but slightly accurately estimated the values of the ASFR for the reproductive ages 44 to 49 years.

Comparison of fitnesses of four models to Ghana's fertility data

In order to compare the fitnesses of models under consideration, all four models have been fitted simultaneously to various annual fertility data of Ghana. The results are shown in Figure 18 *A* and *B*.

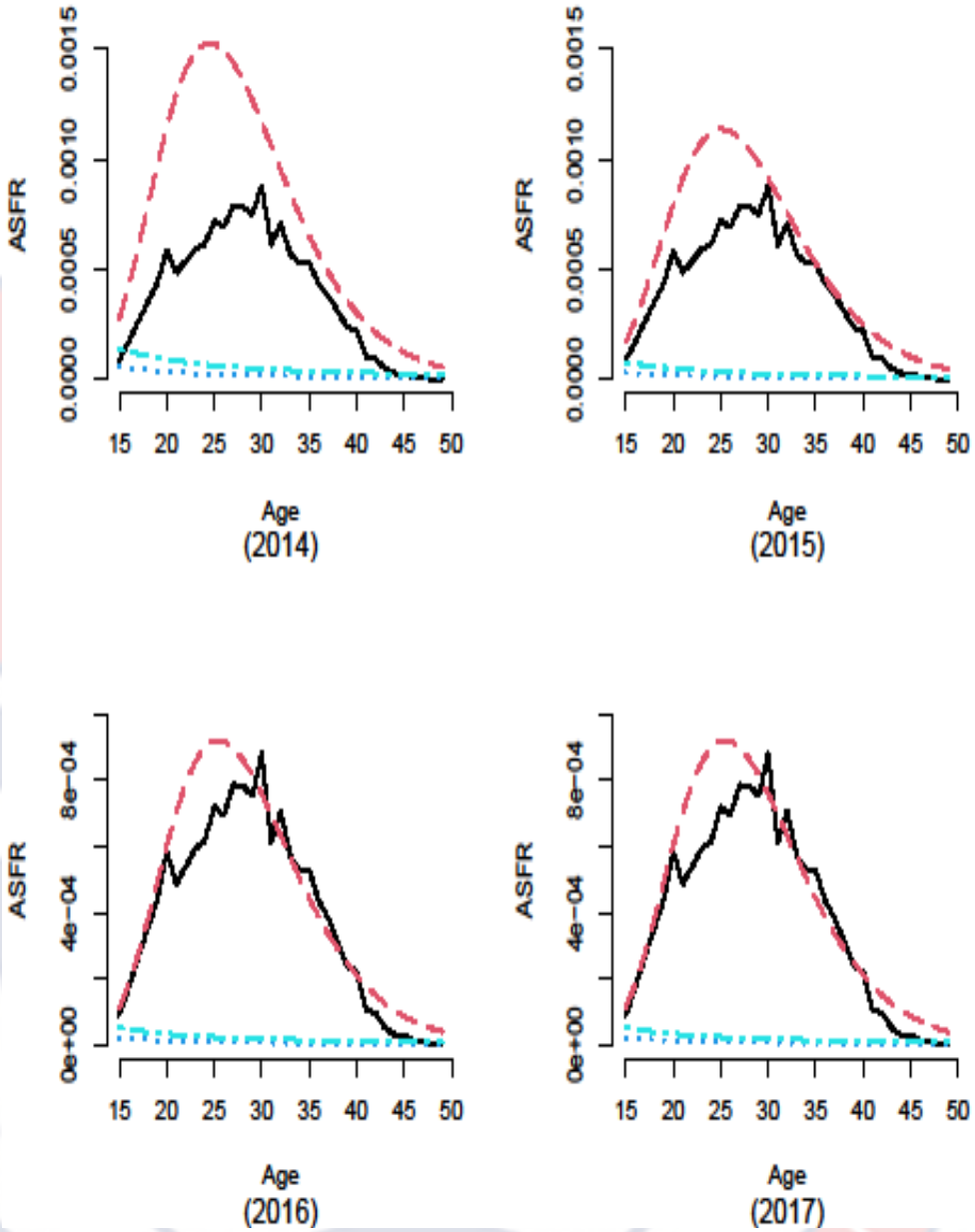

Figure 18 A: Plots of three fitted models and actual ASFR for the years 2014 to 2017 of Ghana.

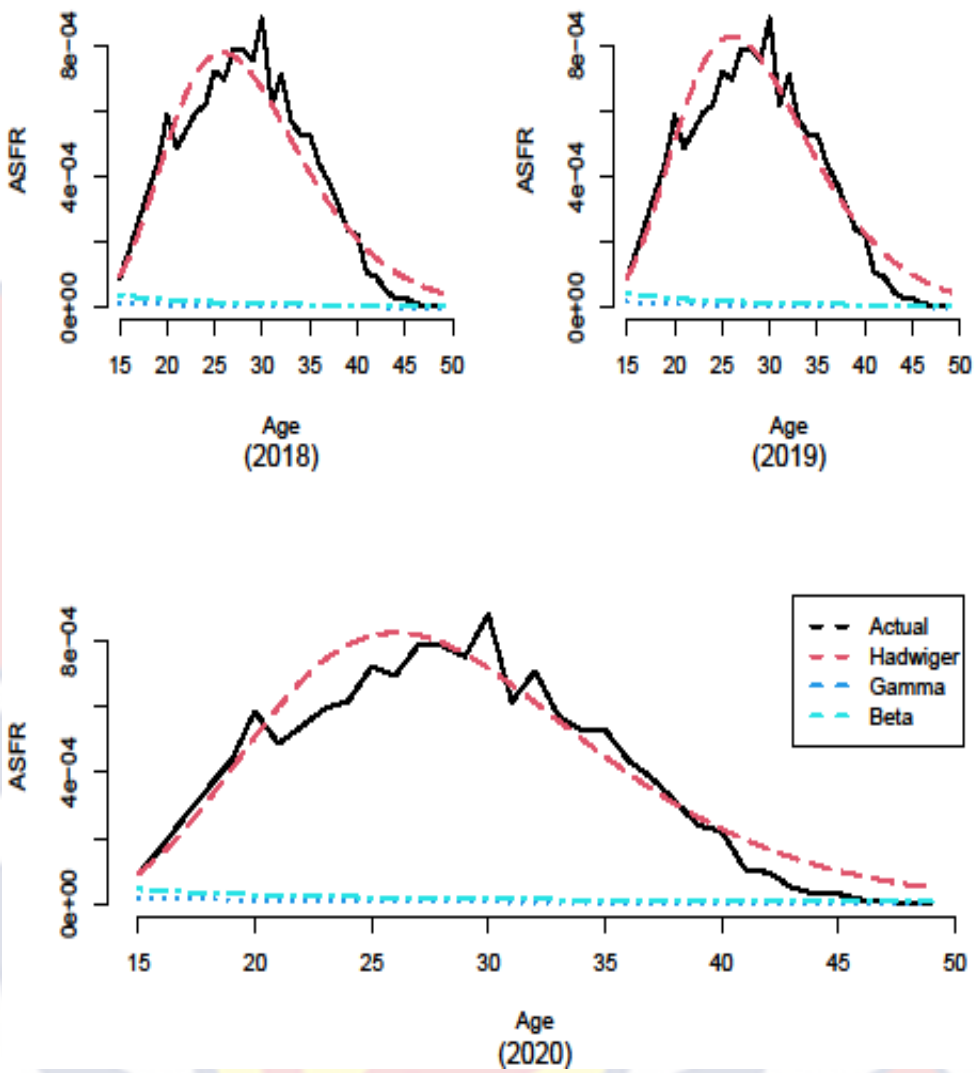

Figure 18 B: Plots of three fitted models and actual ASFR for the years 2018 to 2020 of Ghana

The results show that, not all the models have a good fit for the yearly fertility data of Ghana. Specifically, only the Hadwiger model is seen to fairly fit the distribution of the fertility of Ghana, since it has a much similar curve to the observed ASFRs. Again, for both the Gamma and Beta models, fertility was fairly uniformly distributed over women in the reproductive age groups. Fertility rate was a bit high at an early age (15 years) but declined almost at a fixed level close to zero to the completion of reproductive age period (49 years). Thus, both models largely under estimates Ghana's fertility.

Figure 19 displays the fitnesses of the four selected models to aggregated ASFRs for the period 2014 – 2020.

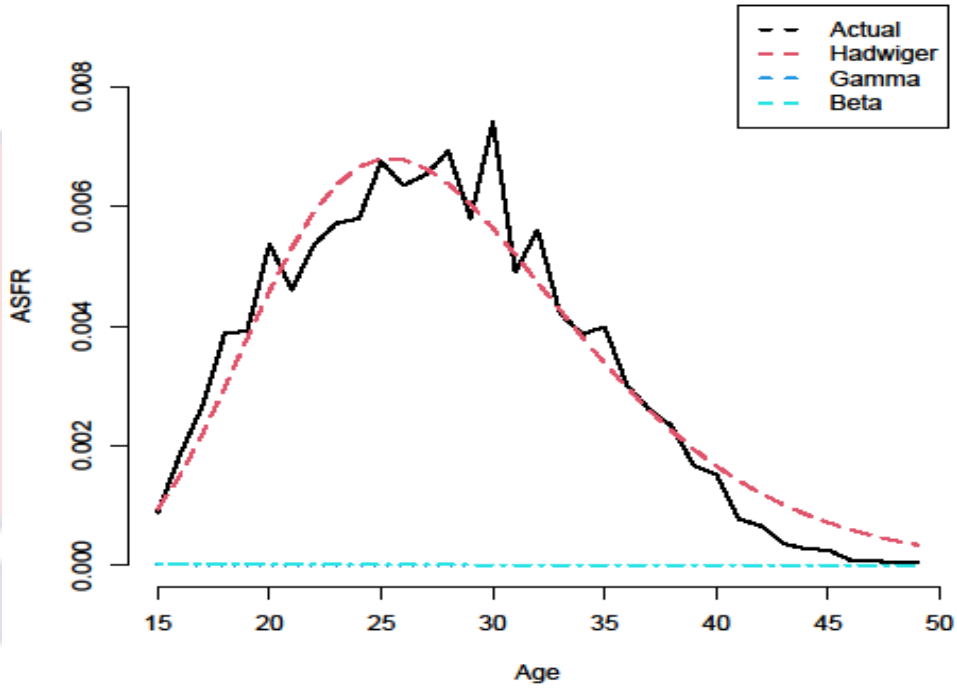

Figure 19: Fertility curves from various models for the period 2014 – 2020.

The distribution of Ghana's fertility for the period 2014 – 2020 is the same as those of the specific years. The distribution of fertility based on the Hadwiger model follows that of the ASFR for the period. The distributions of fertility from other two models considerably depart from the underlying distribution. The Hadwiger model's predicted values for the ASFRs are very similar to the actual ASFR for the period 2014 – 2020. In comparison with the actual ASFRs for mothers aged 15 to 46, both the Gamma and Beta models underestimates fertility, but both models accurately estimate the values of ASFR for mothers aged 47 to 49.

Determining the Best Model for Ghana's Fertility Data

So far, the graphical representations indicate that only the Hadwiger model appropriately fits the fertility data of Ghana. For the purpose of selecting the model that best fits Ghana's fertility data, three popular formal model selection criteria – Sum of Square Error (SSE), Akaike's Information Criteria (AIC), and Corrected Akaike's Information Criteria (AICc) – are employed. The results are presented in Table 2.

Table 3: Model Selection Criteria

Model	No. of Parameters	SSE	AIC	AICc
Hadwiger	3	1.91E-07	-656.813	-656.039
Gompertz	3	1.14E-03	-433.077	-432.303
Gamma	4	7.73E-05	-524.154	-522.821
Beta	5	7.46E-05	-522.250	-520.181

Source: Researcher's own computation, (2022)

The results show that, the Hadwiger model has the smallest value for the sum of square error (SSE). Also, the model has the lowest value for both the AIC and AICc compared to the other three fertility models. Thus, the Hadwiger model is adjudged the best-fitted model for Ghana's fertility data.

In the subsequent sections, Ghana's fertility is forecasted for three years – 2021, 2022, and 2023 – based on actual ASFRs.

Application of Time Series Analysis on the Actual ASFRs of Ghana

To accurately forecast a given time series, it is appropriate to identify a suitable model that underlies the series. An initial important step is to visualize

the pattern of movement of the series in a time series plot. Figure 20 presents time series plots of actual ASFR with corresponding Autocorrelation Function (ACF) and Partial Autocorrelation Function (PACF).

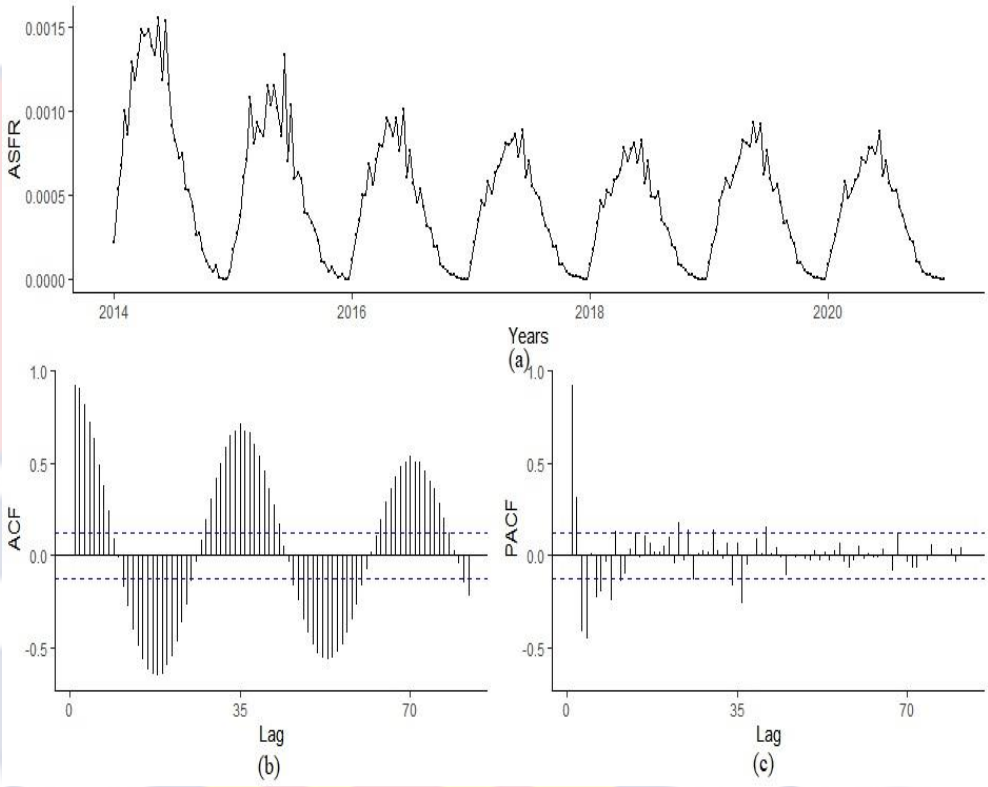

Figure 20: Time series plot of (a) ASFR, (b) ACF and (c) PACF

From Figure 20, it is noticeable that fertility was quite high at the beginning of the period (2014 and 2015), but gradually slows down to almost fixed level over the years. There appears to be a decreasing trend in fertility within the period. It can be observed that fertility seem to be influenced by seasonal effects; lowest fertilities at both the beginning and end of the reproductive period, but highest fertility during the middle of the fecundity period. The figure indicates that, generally the ASFRs are characterized by fluctuations; notably, there were high fluctuations at the initial years but as the level of the series increase the fluctuations tend to die out. In a nutshell, there is a bit of non-stationarity in the ASFRs as the level of the series increases.

To understand further the nature of the ASFRs, the autocorrelation function (ACF) and partial autocorrelation function (PACF) for the series are examined. The results in Figure 20 (b) indicate that, the ACFs are significant at almost all lags, whiles in Figure 20 (c) the PACFs are significant at lag four (4). The ACF also indicates that the data is not stationary and possess some seasonal variation.

In order to address the non-stationarity and seasonal effects in the ASFRs, some kind of differencing needs to be performed on the series. In what follows, a check is done to determine the suitable order for the differencing.

Checking for order of differencing to produce stationarity

The syntaxes nsdiff ( ) and ndiff ( ) in R (Hyndman et al., 2020) statistical software are respectively utilised to determine the numbers of seasonal differencing and regular differencing required for the series to be stationary.

Table 3 shows the results of the numbers of seasonal differencing and regular differencing required to attain stationarity.

Table 4: Number of differencing Required to Attain Stationarity

Type of Differencing	No. of Differencing Required
Seasonal Differencing	1
Regular Differencing	1
Other Difference Required Again	0

Source: Researcher's own computation, (2022)

The results indicate that, the series need to be seasonally differenced once in order to remove the seasonal component. Again, the series should be differenced once to remove the trend component. Further, the results show that after the first order differencing of the series, there is no other differencing required to produce stationarity.

Figure 21 shows the plots of the series, ACF and PACF after first order seasonal differencing of the series.

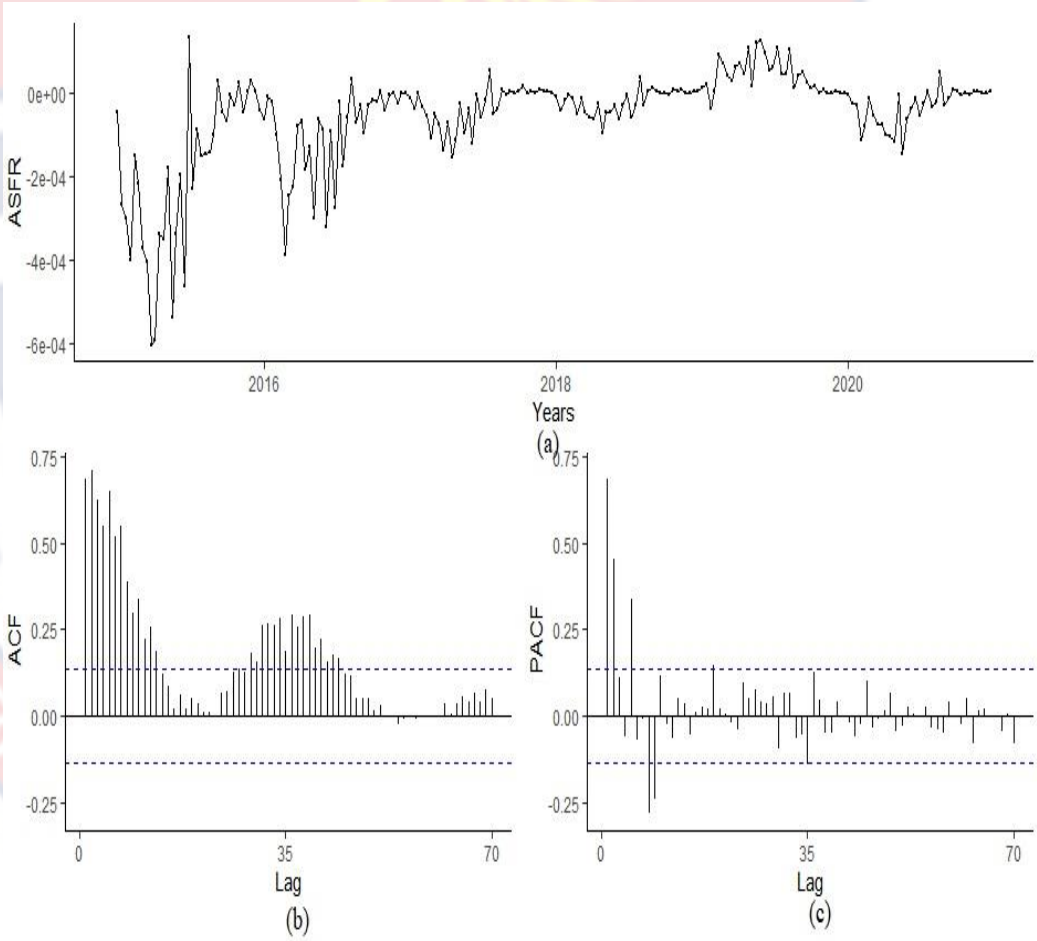

Figure 21: Plots of seasonally differenced (a) ASFR, (b) ACF, and (c) PACF

The results show that the seasonal effects have been reduced, but the series appears not completely stationary. It can be observed from Figure 21 (b) that the ACFs decay rapidly moves towards zero with many significant lags. This is indicative that a moving average process of order one, MA(1), is appropriate for modelling the ASFRs. Moreover, Figure 21 (c) shows that there are significant PACFs at lags one and two, followed by two non-significant PACFs, and thereafter there appears to be some inconsistent significant PACFs, which may be attributed to unusual occurrences. The Figure 21(c) suggests that an autoregressive process of order two, AR(2), is sufficient to model the ASFRs.

Figure 22 presents the results of combined seasonal and regular differencing of the series.

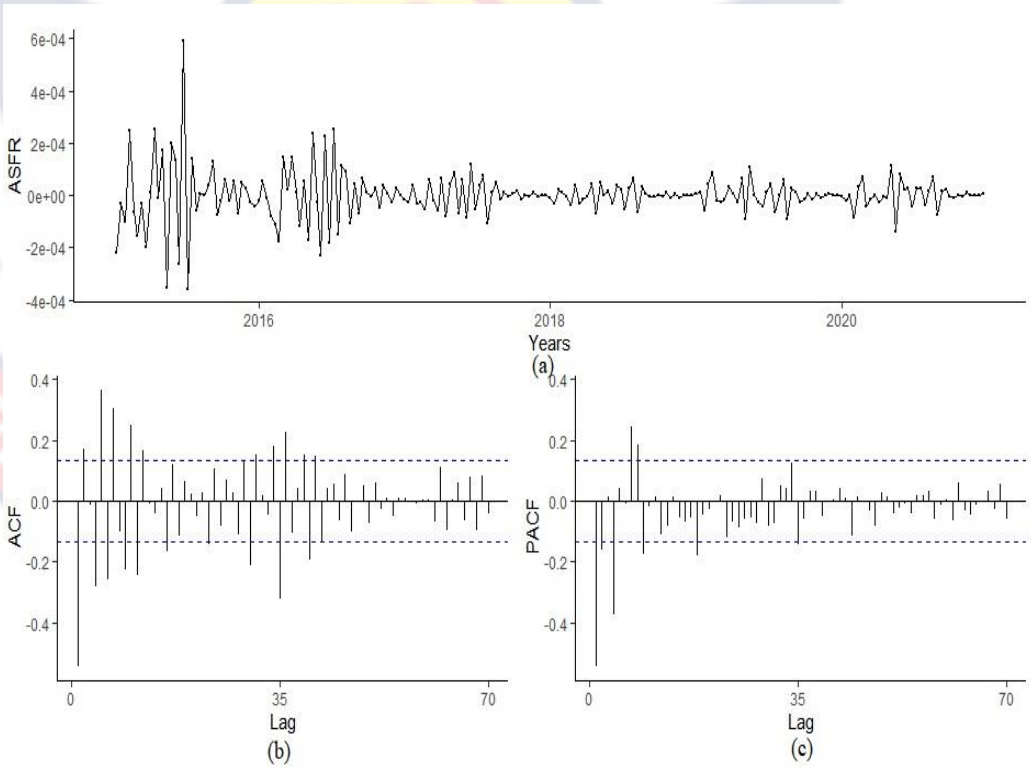

Figure 22: Plots of combined seasonal and regular differenced series with corresponding correlograms

Figure 22 (a) shows that, after taking the combined seasonal and regular differencing, the series have become fairly stationary though with some unusual occurrences at the beginning of the period. The figure shows that both the ACF (Figure 22 (b)) and PACF (Figure 22 (c)) plots possess significant spikes, constituting less than 5%, at some lags. The combined seasonal and regular differenced ASFRs are more stable, and thus, become appropriate for modelling.

Model selection for forecasting

Various autoregressive integrated moving average (ARIMA) models that incorporate seasonal effects have been examined in relation to ASFRs for the purpose of selecting the most plausible forecasting model. The study utilizes the AIC value as the criterion for selecting the so-called best model. Table 4 presents various SARIMA$(p,d,q)(P,D,Q)_S$ models with corresponding AIC values.

Table 5: Different Types of SARIMA Models with AIC Values

No.	Model Type	AIC Value
1	SARIMA$(2,1,1)(0,1,2)_{35}$	-3395.024
2	**SARIMA$(2,1,1)(0,1,1)_{35}$**	**-3396.174**
3	SARIMA$(4,1,0)(0,1,1)_{35}$	-3398.944
4	SARIMA$(4,1,1)(1,1,0)_{35}$	-3397.451

Source: Researcher's own computation, (2022)

The results show that, although Model 3 has the lowest AIC value, comparatively, there are no substantial differences among the AIC values for all

four candidate models. In this case, the AIC is deemed unsuitable criterion for selecting the best model. However, based on the principle of parsimony, Model 2, that is, SARIMA(2,1,1)$(0,1,1)_{35}$, is selected as most plausible for forecasting the ASFRs as it contains few parameters compared to the other candidate models. The model indicates a non-seasonal AR(2) and no seasonal AR component, first regular and seasonal differencing, and non-seasonal and seasonal MA(1) component. In addition, the model shows a seasonal order of 35, which is the number of observations per year. In this case, the observations (that is, seasonal length) are the distinct ages of women in the reproductive period.

Table 5 shows the estimated SARIMA$(2,1,1)\times(0,1,1)_{35}$ model for the ASFRs.

Table 6: Estimated SARIMA$(2,1,1)(0,1,1)_{35}$ Model

Model	Estimate	Std Error	2.5% CI	97.5% CI
AR1	-1.2918	0.1084	-1.5043	-1.0793
AR2	-0.5140	0.0687	-0.6487	-0.3793
MA1	0.7288	0.1071	0.5188	0.9388
SMA1	-0.4777	0.0801	-0.6346	-0.3208

Source: Researcher's own computation, (2022)

The results show that the parameter AR2 had the lowest standard error among all the other parameters, while the parameter AR1 had the highest standard error. The results indicate that all the estimated parameters of the SARIMA$(2,1,1)(0,1,1)_{35}$ model are statistically significant since their corresponding confidence intervals do not contain zero.

After the parameters of the model have been estimated, the model needs to be checked to determine if it satisfies the assumptions of seasonal ARIMA model. Thus, the residuals of the model must follow a white noise process having mean zero, constant variance, and uncorrelated.

Model diagnostics

The diagnostic test is used to check the correlation and significance of the residuals. That is, whether the residuals are white noise or not. Figure 23 displays the results of validation of the SARIMA(2,1,1)$(0,1,1)_{35}$ model.

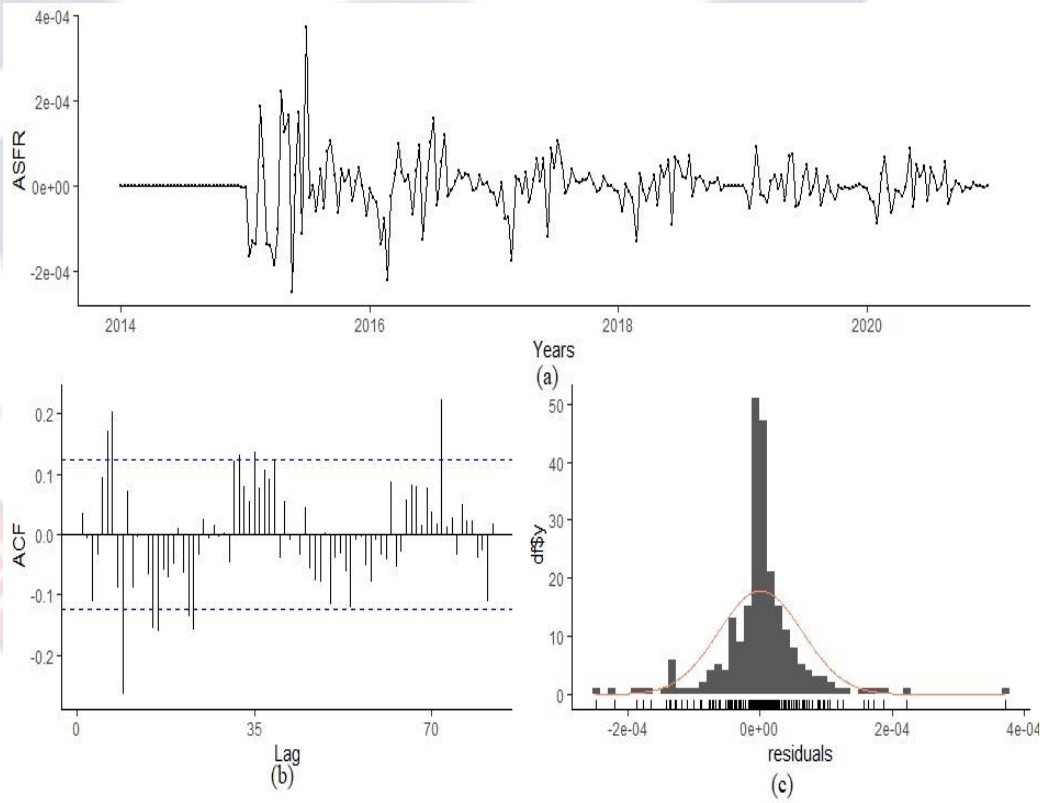

Figure 23: Plots of (a) fitted SARIMA(2,1,1)(0,1,1)35 model, (b) ACF and (c) residuals

The results show that the fitted series hovers around a fixed mean of zero, and its variation seem not depend on the level of the series as evident in Figure 23 (a). Figure 23 (b) shows that all the autocorrelations are not significant, except at few lags. The few significant lags on the ACF is as a result of the seasonal effects. Moreover, the plot for the residuals in Figure 23 (c) shows that the residuals are normally distributed. These indicate that the SARIMA$(2,1,1)(0,1,1)_{35}$ model is appropriate for the series.

In what follows, the Ljung-Box test is carried out to confirm, or otherwise, that the residuals are indeed a white noise process.

Ljung-Box test for serial correlation among the residuals

The results of the test for serial correlation among the residuals are based on the following hypothesis:

H_0 : There is no serial correlation among the residuals; against

H_1 : There is a serial correlation among the residuals.

Table 6 displays the results of the Ljung-Box test.

Table 7: Ljung-Box Test for Serial Correlation of Residuals

Statistic	Chi-Square	Df	*P*-Value
Value	118.47	45	0.5792

Source: Researcher's own computation, (2022)

The results in the table show that, the test for serial correlation among residuals is not significant at 5% level of significance. In this case, we fail to reject the null hypothesis (H_0), which states that there is no serial correlation among the residuals. Therefore, the study concludes that the residuals from the

SARIMA$(2,1,1)(0,1,1)_{35}$ model are a purely random process, implying the appropriateness of the model.

Forecasting the fertility rates of Ghana

The section presents the results of forecasting the fertility of Ghana for three consecutive years, namely 2021, 2022 and 2023. The fertility forecasts are obtained from the SARIMA$(2,1,1)(0,1,1)_{35}$ model using actual ASFR values for the year 2020 as reference. The forecasts are shown in Figure 24.

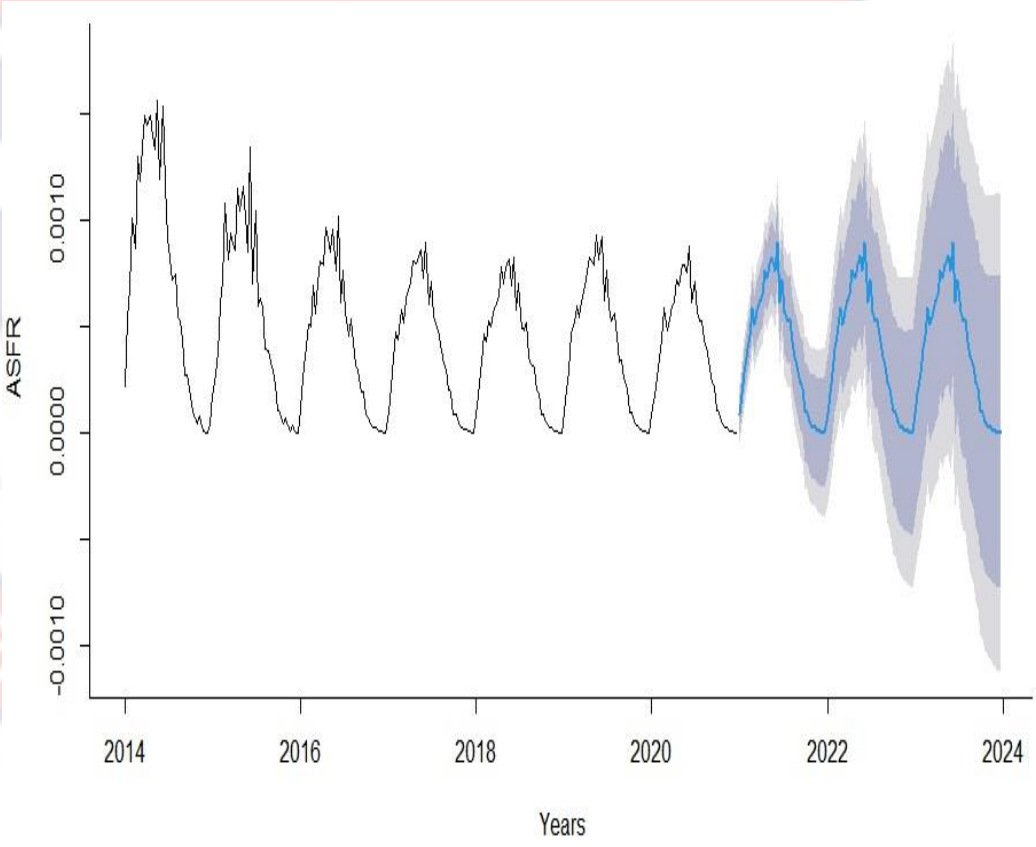

Figure 24: Plot of actual and forecasted ASFRs of Ghana

The results show that forecasted ASFRs followed suit as the actual ASFR. The results reveal that Ghana's fertility rate will continue to decline in the next few years.

The distributions of the actual ASFRs for the year 2020, and forecasted ASFRs for the years 2021, 2022, and 2023 are presented in Figure 25.

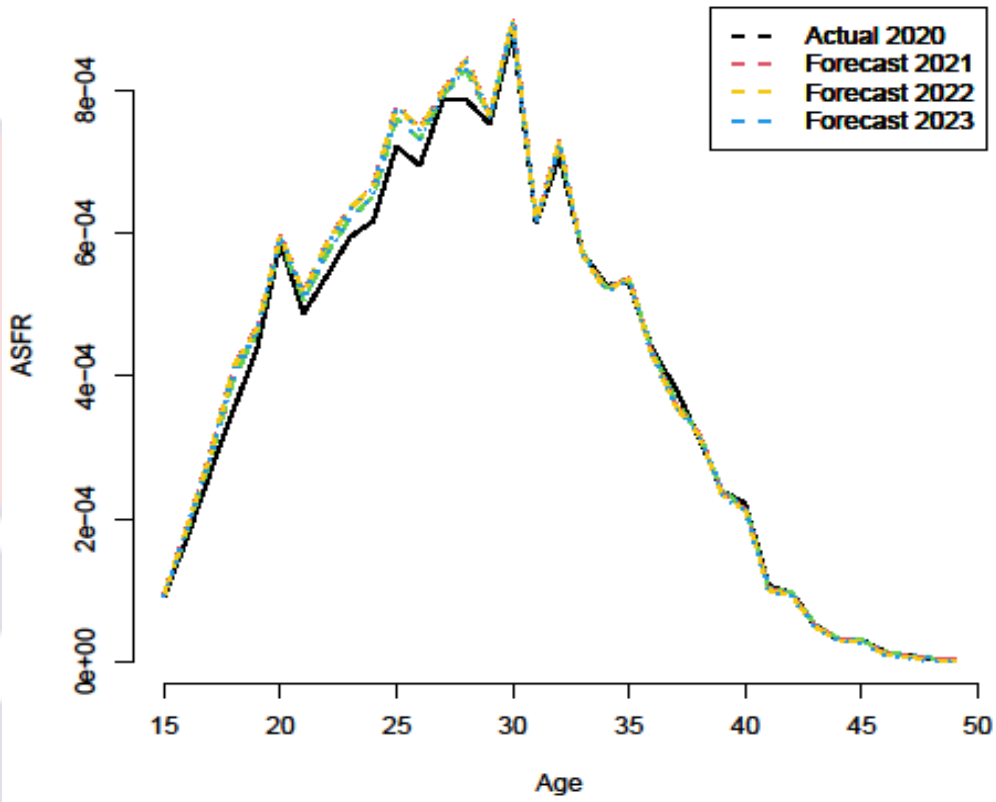

Figure 25: Plots of actual, fitted and forecasted ASFRs of Ghana

The results show that the forecasted fertility curves closely follow the underlying distribution of the fertility rates of Ghana. The figure indicates that estimated fertility rates for the years 2021, 2022, and 2023 appear to be higher than the actual ASFRs for the year 2020 for women in the first half of reproduction period. In this case, projected fertility rates are higher among women below the age of about 30 years. In a broader perspective, it can be seen that in the years, fertility peaks among women in the 25 – 30 age category.

Table 6 presents forecasted ASFRs for the years 2021, 2022, and 2013 for various age groups of women in the reproduction period.

Table 8: Forecasted ASFRs for the years 2021, 2022, and 2013 for Various age Groups of Women

Age Group	Actual ASFR	Forecasted ASFRs		
	2020	2021	2022	2023
15 – 19	1.32E-03	1.46E-03	1.45E-03	1.45E-03
20 – 24	2.82E-03	3.00E-03	3.00E-03	2.99E-03
25 – 29	3.74E-03	3.93E-03	3.93E-03	3.92E-03
30 – 34	3.30E-03	3.34E-03	3.33E-03	3.32E-03
35 – 39	1.90E-03	1.88E-03	1.87E-03	1.86E-03
40 – 44	5.06E-04	4.91E-04	4.84E-04	4.77E-04
45 – 49	6.39E-05	5.59E-05	4.90E-05	4.21E-05

Source: Researcher's own computation

The table indicates that forecasted ASFRs are marginally higher than the actual ASFRs for the year 2020. The results show that, for the women in the 15 – 19 reproductive age group, there were 132 live births per 100,000 women in 2020, an estimated 146 live births per 100,000 women for the year 2021, 145 live births per 100,000 women for the year 2022, and 145 live births per 1,000 women for the year 2023. Also, the results indicate that, for women in the 45 – 49 age group, there were 639 live births per 10,000,000 women in 2020, a predicted 559, 490, and 421 live births per 10,000,000 women for the years 2021, 2022, and 2023 respectively. In the next few years, fertility will attain its highest in 25 – 29 reproductive age group. Specifically, there will be 393, 393, and 392 live births per 100,000 women for the respective years 2021, 2022, and 2023.

Chapter Summary

In the chapter, the study explored Ghana's fertility data for the period 2014 to 2020 using descriptive statistics and fertility curves. The results show that the distribution of Ghana's fertility is positively skewed. The study reveals that, for the period under consideration, there is a decline in the fertility rate of Ghana.

Subsequently, the data was assessed base on four standard fertility models, namely the Hadwiger, Gompertz, Gamma, and Beta. The results reveal that only the Hadwiger model fits the distribution of the Ghana's fertility data adequately. However, the results show that the other three fertility models, Gompertz, Gamma and Beta, considerably depart from the underlying distribution of the fertility of Ghana.

Finally, time series analysis was performed on the best-fitted model (i.e., the Hadwiger model) in order to forecast the ASFRs of Ghana's for the period 2021 – 2023. The results reveal that there is presence of both downward trend and seasonality in the ASFRs of Ghana. To appropriately model the series, each of regular differencing, and combined regular and seasonal differencing were performed once on the ASFRs to obtain stationarity. The results reveal that SARIMA$(2,1,1)(0,1,1)_{35}$ model fits the differenced series well. The model is found to be valid, and adjudged good for forecasting, since there is no serial correlation among its residuals. Forecasted values for the period 2021 – 2023 indicate that the ASFRs of Ghana will continue to decline on yearly basis with highest fertility rate occurring among women in the 25 – 29 reproduction years.

CHAPTER FIVE

SUMMARY, CONCLUSIONS, AND RECOMMENDATIONS

Overview

This final chapter presents a summary of the study's findings. Also, some conclusions based on the findings of the study have been drawn and recommendations made.

Summary of the Study

The study generally models the age-specific fertility rate of Ghana. The study is based on fertility data that spans from the years 2014 – 2020. Three standard fertility models – the Hadwiger, Gamma, and Beta – are fitted to the data with the view of selecting the best model.

The study explored Ghana's fertility data for the period 2014 – 2020. For the period under study, the year 2014 had the highest mean number of births (73) per 100,000 women, which decreased on yearly basis, with the year 2018 recording the lowest mean value (about 39). In the year 2018, the number of live births ranged between about 28 and 83 per 100,000 women. Overall, there were 332 live births per 100,000 women across all age groups for the period 2014 – 2020. In the period, number of live births lingered between about 41 per 1,000,000 women and 741 per 100,000 women. The results show that the distribution of Ghana's fertility is positively skewed. The study reveals that, for the period under consideration, there is a decline in the fertility rate of Ghana.

Subsequently, the data was assessed base on the Three standard fertility models. The results reveal that only the Hadwiger model fits the distribution of the Ghana's fertility data adequately. However, the results show that the other

two fertility models, Gamma and Beta, considerably depart from the underlying distribution of the fertility of Ghana.

Time series analysis was performed on the best fitted model (i.e., the Hadwiger model) in order to forecast the ASFRs of Ghana's for the period 2021 – 2023. The results reveal that there is both downward trend and seasonality in the ASFRs of Ghana. To appropriately model the series, each of regular differencing, and combined regular and seasonal differencing were performed once on the ASFRs to obtain stationarity. The results reveal that SARIMA$(2,1,1)(0,1,1)_{35}$ model fits the differenced series well. The model is found to be valid, and adjudged good for forecasting, since there was no serial correlation among its residuals. Forecasted values for the period 2021 – 2023 indicate that the ASFRs of Ghana will continue to decline on yearly basis with highest fertility rate occurring among women in the 25 – 29 reproduction years.

Conclusions

The study successfully reviews three standard fertility models, namely the Hadwiger, Gamma and Beta model. The study finds that various parameters of the models directly influence fertility distributions.

Additionally, the study has established that the distribution of Ghana's fertility pattern is positively skewed. A significant observation in the study is that there is, on yearly basis, continuous decline in the fertility rate of Ghana. Ghana's fertility is highest among women in the 25 – 30 reproductive ages.

The study finds the Hadwiger model most suitable for modelling Ghana's fertility data. In this case, the Hadwiger fertility model closely follows and fairly fit the underlying distribution of the fertility of Ghana.

The study projects that for the period 2021 – 2023 ASFRs of Ghana will continue to decrease with highest fertility rate occurring among women in the 25 – 29 reproduction years.

Recommendations

The study noted that various parameters of fertility models directly influence fertility distributions. In view of this, it is of great importance to consider suitable procedures in estimating the values of these model parameters.

The study is of the view that Government and its agencies, the National Population Council, National Development Commission, private organisations and non-governmental organisations, and other planners and policy makers adopts the Hadwiger fertility model in their quest to estimate various fertility rates of Ghana for planning and decision-making process.

The study points out that fertility rates of Ghana decrease yearly, and the pattern is projected to continue in the next few years. To this end, the study recommends further investigation into factors that influence the decline in fertility rate of Ghana.

REFERENCES

Abramowitz, M., & Stegun, I. A. (Eds.). (1964). *Handbook of mathematical functions with formulas, graphs, and mathematical tables* (Vol. 55). US Government printing office.

Akaike, H. (1974). A new look at the statistical model identification. IEEE transactions on automatic control, *19*(6), 716-723.

Akoth, O. E. (2017). Modeling the Effects of Interference in Fertility Rate of Kenya. *Journal of Mathematics and Statistical Science*, *11*, 322-334.

Apergis, N., Mervar, A., & Payne, J. E. (2017). Forecasting disaggregated tourist arrivals in Croatia: Evidence from seasonal univariate time series models. *Tourism Economics*, *23*(1), 78-98.

Aryee, A.F. (1985). "Nuptiality Patterns in Ghana." In Demographic Patterns in Ghana: Evidence from the Ghana Fertility Survey 1979/80, ed. S.Singh, J.Y. Owusu, and I.H. Shah. Voorburg, Netherlands: International Statistical Institute.

Aviisah, P. A., Dery, S., Atsu, B. K., Yawson, A., Alotaibi, R. M., Rezk, H. R., & Guure, C. (2018). Modern contraceptive use among women of reproductive age in Ghana: analysis of the 2003–2014 Ghana Demographic and Health Surveys. *BMC women's health*, *18*(1), 1-10.

Ayad, M., & Roudi, F. (2006). Fertility declines and reproductive health in Morocco: New DHS figures. *Washington, D.C.: Population Reference Bureau*, 1-4

Bermúdez, S., Blanquero, R., Hernández, J. A., & Planelles, J. (2012). A new parametric model for fitting fertility curves. *Population Studies*, *66*(3), 297-310.

Blanc, A. K., & Grey, S. (2002). Greater than expected fertility decline in Ghana: untangling a puzzle. *Journal of Biosocial Science*, *34*(4), 475-495.

Bongaarts, J. (2015). Modeling the fertility impact of the proximate determinants: Time for a tune-up. *Demographic Research*, *33*, 535-560.

Bosomprah, J. (2008). Contextual Issues Affecting the Use of Contraceptives among Women in the Offinso District, Ghana (Doctoral dissertation).

Caldwell, J. C. (1980). Mass education as a determinant of the timing of fertility decline. *Population and development review*, 225-255.

Calverton, M. (2008). USA: GSS, GHS, & Macro International; 2009. 20 Ghana Statistical Service (GSS), Ghana Health Service (GHS), and ICF Macro. *Ghana Demographic and Health Survey*.

Chandiok, K., Mondal, P. R., Mahajan, C., & Saraswathy, K. N. (2016). Biological and Social Determinants of Fertility Behaviour among the Jat Women of Haryana State, India. *ratio (CWR)*, *368*, 186-1.

Crissman, H. P., Engmann, C. E., Adanu, R. M., Nimako, D., Crespo, K., & Moyer, C. A. (2013). Shifting norms: pregnant women's perspectives on skilled birth attendance and facility–based delivery in rural Ghana. *African journal of reproductive health*, *17*(1), 15-26.

Davis, C. P. (2021). Definition of fertility. WebMD,LLC. Rxlist, retrieval December, 14, 2021. https://www.rxlist.com/fertility/definition.htm

Deb, M., & Chakrabarty, T. K. (2016). Functional time series analysis of age-specific fertility rates: Visualizing the change in the age-pattern of fertility in India. *International Journal of Advanced Statistics and Probability,4(2),* 79-89.

Dockalova, B., Lau, K., Barclay, H., & Marshall, A. (2016). Sustainable development goals and family planning 2020. *The International Planned Parenthood Federation (IPPF). United Kingdom*, 1-12.

Fage, J. D., Davies, O, Maier, D. J. & Boateng, E. A. (2021). Ghana. Encyclopedia Britannica. https://www.britannica.com/place/Ghana

Fertilitynetworkuk, (n.d), Factors Affecting Fertility, retrieved July, 15, 2021, from https://fertilitynetworkuk.org/fertility-faqs/factors-affecting-fertility/

Gabrysch, S., Cousens, S., Cox, J., & Campbell, O. M. (2011). The influence of distance and level of care on delivery place in rural Zambia: a study of linked national data in a geographic information system. *PLoS medicine*, *8*(1), e1000394.

Gayawan, E., & Ipinyomi, R. A. (2009). A comparison of Akaike, Schwarz and R square criteria for model selection using some fertility models. *Australian Journal of Basic and Applied Sciences*, *3*(4), 3524-3530.

Gayawan, E., Adebayo, S. B., Ipinyomi, R. A., & Oyejola, B. A. (2010). Modeling fertility curves in Africa. *Demographic Research*, *22*, 211-236.

Gebremeskel, H. G. (2016). Implementing hierarchical bayesian model to fertility data: the case of Ethiopia. *Padua Research Archive, Ciclo 28*, 567.

GSS, GHS & ICF Macro (2009) Demographic and Health Survey 2008. Calverton, Maryland: Ghana Statistical Service, Ghana Health Service and ICF Macro.

Ghana. Statistical Service, & ORC Macro. (2009). *Ghana demographic and health survey, 2008*. Ghana Statistical Service.

Ghana Statistical Service. (2014). 2010 Population & Housing Census Report: *Disability in Ghana*. Ghana Statistical Service.

Gupta, A., & Pasupuleti, S. S. R. (2013). A new behavioural model for fertility schedules. *Journal of Applied Statistics*, *40*(9), 1921-1930.

Halim, S., & Bisono, I. N. (2008). Automatic seasonal auto regressive moving average models and unit root test detection. *International Journal of Management Science and Engineering Management*, *3*(4), 266-274.

Hamilton, J. D. (1994). Time Series Analysis (Princeton University Press, Princeton, NJ) ISBN 0-691-04289-6. *International Journal of Forecasting*.

Hoem, J. M., Madsen, D., Nielsen, J. L., Ohlsen, E. M., Hansen, H. O., & Rennermalm, B. (1981). Experiments in modelling recent Danish fertility curves. *Demography*, *18*(2), 231-244.

Hurvich, C. M., & Tsai, C. L. (1989). Regression and time series model selection in small samples. *Biometrika*, *76*(2), 297-307.

Hyndman, R. J., & Khandakar, Y. (2008). Automatic time series forecasting: the forecast package for R. *Journal of statistical software*, *27*, 1-22.

Hyndman, R. J., & Athanasopoulos, G. (2018). Forecasting: principles and practice, OTexts: Melbourne, Australia. OTexts. com/fpp2.

Hyndman, R. J., Athanasopoulos, G., Bergmeir, C., Caceres, G., Chhay, L., O'Hara-Wild, M., ... & Wang, E. (2020). Package 'forecast'. *Online] https://cran. r-project. org/web/packages/forecast/forecast. pdf*.

Mathivanan, N. M. N, Ghani, Ab. P., & Ghani, Md. N. A. (2018). Tracing Mathematical Function of Age Specific Fertility Rate in Peninsular Malaysia. Indonesian Journal of Electrical Engineering and Computer Science. 9. 637-642. 10.11591/ijeecs.v9.i3.pp637-642.

McDonald, P. F. (1984). Nuptiality and completed fertility: a study of starting, stopping and spacing behaviour. *International Statistical Institute*.

McNown, R., & Rajbhandary, S. (2003). Time series analysis of fertility and female labor market behavior. *Journal of Population Economics, 16*, 501-523.

Melkersson, M., & Rooth, D. O. (2000). Modeling female fertility using inflated count data models. *Journal of Population Economics*, *13*(2), 189-203.

Mishra, R. K., & Upadhyay, S. K. (2019). Parametric Bayes Analyses to Study the Age-Specific Fertility Patterns. *American Journal of Mathematical and Management Sciences*, *38*(2), 151-173.

Mishra, R., Singh, K. K., & Singh, A. (2017). A model for age-specific fertility rate pattern of India using skew-logistic distribution function. *American Journal of Theoretical and Applied Statistics*, *6*(1), 32-37.

Mitra, S. (1967). The pattern of age-specific fertility rates. *Demography*, *4*(2), 894-906.

Moultrie, T. A., Dorrington, R. E., Hill, A. G., Hill, K., Timæus, I. M., & Zaba, B. (2013). *Tools for demographic estimation*. International Union for the Scientific Study of Population.

Nakazawa, M. (2018). fmsb: Functions for medical statistics book with some demographic data. *R package version 0.6*, *3*.

Nations, U. (2015). World Population Prospects: The 2015 Revision, Key Findings and Advance Tables. New York: United Nations, Department of Economic and Social Affairs PD. *Population Division*.

Norville, C., Gomez, R., & Brown, R.L. (2003). Some causes of fertility rates movements. University of Waterloo, *Institute of Insurance and Pension Research.* (Research report 03-02).

http://www.stats.uwaterloo.ca/stats_navigation/IIPR/2003Reports/03-02.pdf.

Nyarko, S. H. (2012). Determinants of adolescent fertility in Ghana. *International Journal of Sciences: Basic and Applied Research*, *5*(1), 21-32.

Oberhofer, W., & Reichsthaler, T. (2004). Modelling fertility: a semi-parametric approach. *Regensburger Diskussionsbeiträge zur*

Wirtschaftswissenschaft, *396*.

Owoo, N. S., Lambon-Quayefio, M. P., & Onuoha, N. (2019). Abortion experience and self-efficacy: exploring socioeconomic profiles of GHANAIAN women. *Reproductive health*, *16*(1), 1-13.

Peristera, P., & Kostaki, A. (2007). Modeling fertility in modern populations. *Demographic Research*, *16*, 141-194.

Population Reference Bureau's, (2011). *World Population Data Sheet' http://www.prb.org/pdf11/2011population-data-sheet_eng.pdf*

Ramos, H. M., Peinado, A., Ollero, J., & Ramos, M. G. (2013). Analysis of inequality in fertility curves fitted by gamma distributions. *SORT: statistics and operations research transactions*, *37*(2), 0233-240.

Sharma, R. K. (2004). *Demography and population problems*. Atlantic Publishers & Dist.

Singh, B. P., Gupta, K., & Singh, K. K. (2015). Analysis of fertility pattern through mathematical curves. *American Journal of Theoretical and Applied Statistics*, *4*(2), 64-70.

Srivastava, U., Singh, K. K., Pandey, A., & Narayan, N. (2021). Experiments in modeling recent Indian fertility pattern. *Scientific reports*, *11*(1), 1-14.

Sychareun, V., Hansana, V., Phengsavanh, A., Chaleunvong, K., & Tomson, T. (2015). Perceptions and acceptability of pictorial health warning labels vs text only-a cross-sectional study in Lao PDR. *BMC Public Health*, *15*(1), 1-10.

Thompson, P. A., Bell, W. R., Long, J. F., & Miller, R. B. (1989). Multivariate time series projections of parameterized age-specific fertility rates. *Journal of the American Statistical Association*, *84*(407), 689-699.

United Nations, Department of Economic and Social Affairs, Population Division (2015). World Population Prospects: The 2015 Revision. New York: United Nations

Vähi, M. (2017). Fertility modelling. *Papers on Anthropology*, *26*(1), 107-114.

Visalakshi, S., & Geetha, R. (2018). Modelling age specific fertility rate in India through fertility curves. *Bulletin of Pure & Applied Sciences-Mathematics and Statistics*, *37*(2), 391-405.

Weisstein, E. W. (2002). Digamma function. From *MathWorld*--A Wolfram Web Resource.

https://mathworld.wolfram.com/DigammaFunction.html

Westoff, Charles F. 2003. Trends in Marriage and Early Childbearing in Developing Countries. DHS Comparative Reports No. 5. *Calverton, Maryland: ORC Macro.*

APPENDICES

APPENDIX A

PARAMETER ESTIMATES OF VARIOUS MODELS

Parameter estimates for the Hadwiger model

Year	A	b	c
2014	0.0149	2.5951	27.4324
2015	0.0112	2.6217	27.9556
2016	0.0090	2.6803	28.2464
2017	0.0083	2.6442	28.6195
2018	0.0079	2.6108	28.7951
2019	0.0084	2.6270	28.9827
2020	0.0081	2.6500	29.3268

Source: Researcher's own computation

Parameter Estimates for Gamma Model

Year	b	C	d	R
2014	28.2279	0.02384	1.79E-04	0.0268
2015	28.7663	0.01792	1.34E-04	0.0202
2016	29.0655	0.0144	1.08E-04	0.0162
2017	29.4495	0.01328	9.96E-05	0.0149
2018	29.6302	0.01264	9.48E-05	0.0142
2019	29.8232	0.01344	1.01E-04	0.0151
2020	30.1773	0.01296	9.72E-05	0.0146

Source: Researcher's own computation

Parameter estimates for Beta model

Year	R	α	β	A	B
2014	0.0270	0.0691	1.60354	0.1788	0.5513
2015	0.0203	0.0520	1.20534	0.1344	0.4144
2016	0.0162	0.0418	0.96858	0.108	0.333
2017	0.0149	0.0385	0.89325	0.0996	0.3071
2018	0.0142	0.0367	0.8502	0.0948	0.2923
2019	0.0151	0.0390	0.90401	0.1008	0.3108
2020	0.0146	0.0376	0.87172	0.0972	0.2997

Source: Researcher's own computation

APPENDIX B

FERTILITY CURVES FOR GAMMA AND BETA MODELS

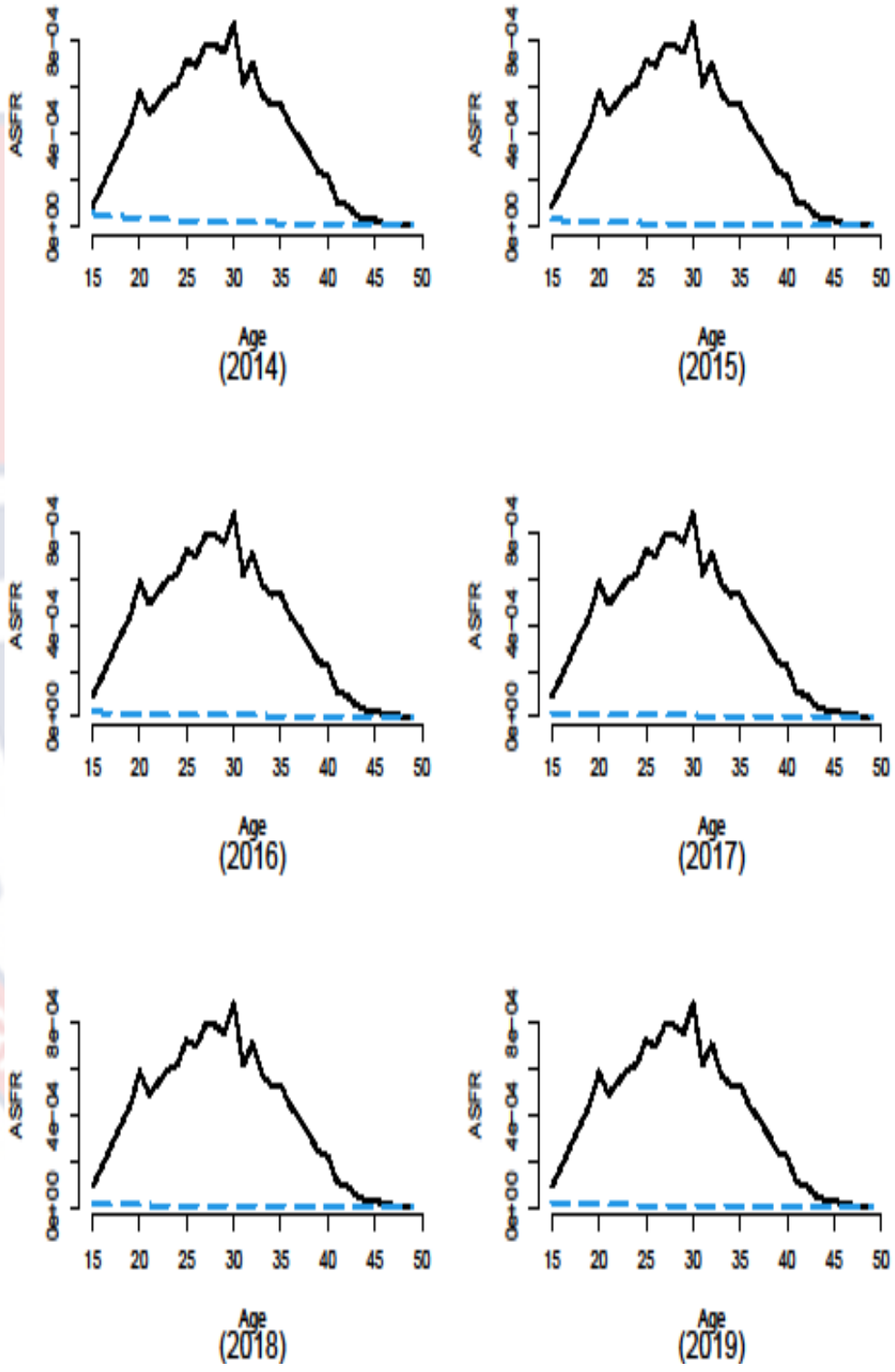

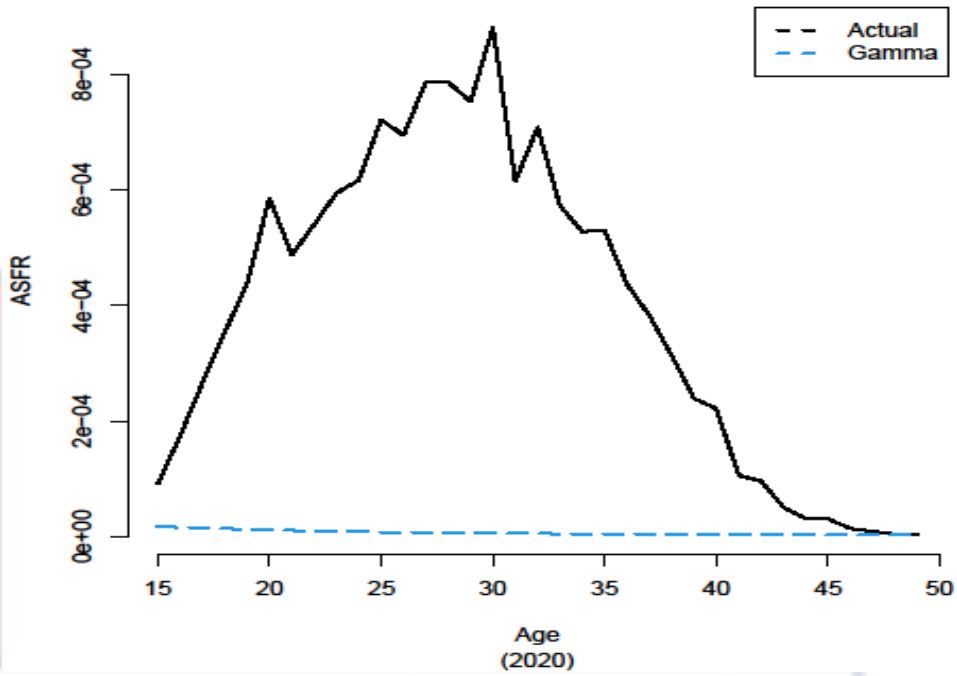

Plots of fitted Gamma model and actual ASFRs for the years 2014 to 2020

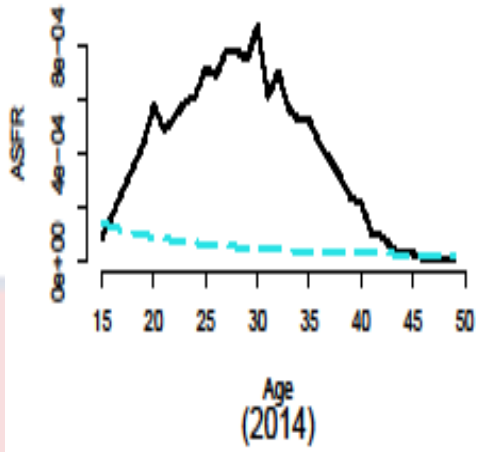

(2014)

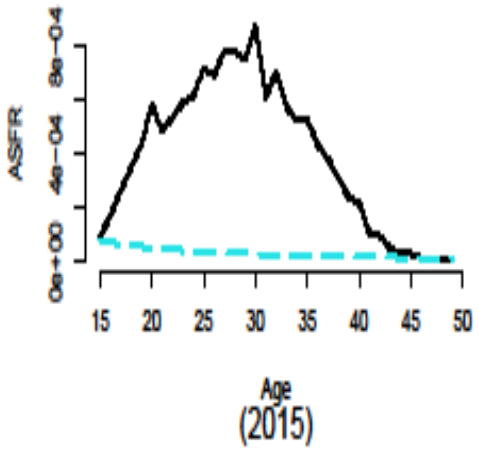

(2015)

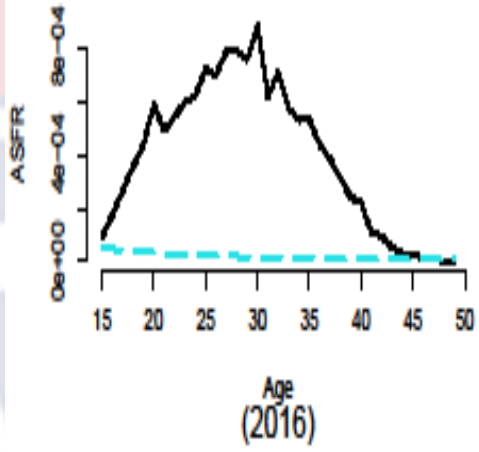

(2016)

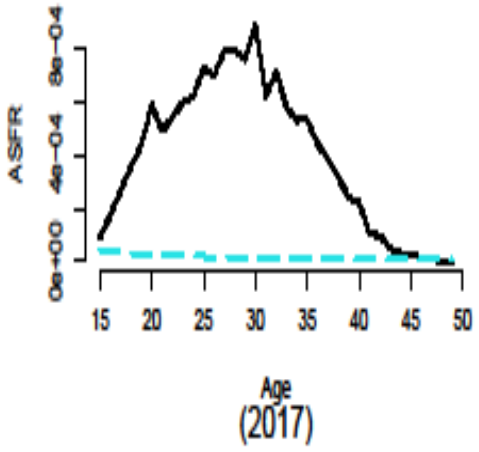

(2017)

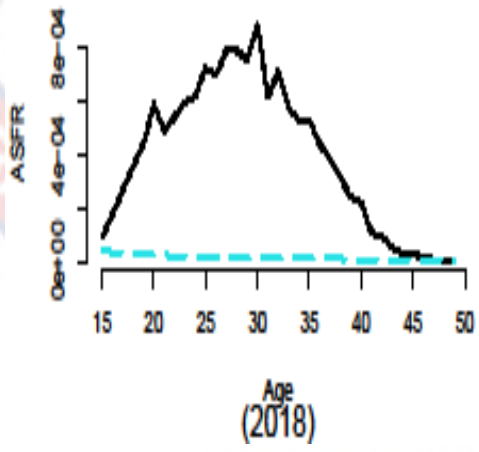

(2018)

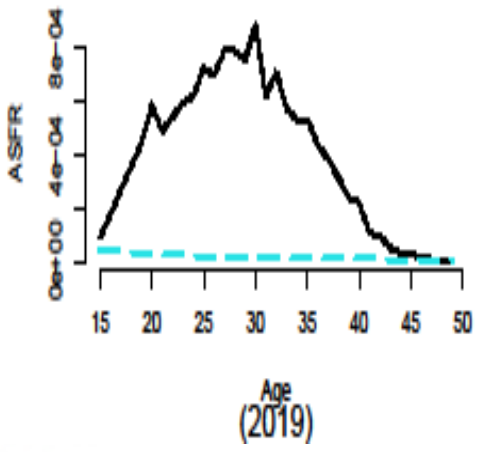

(2019)

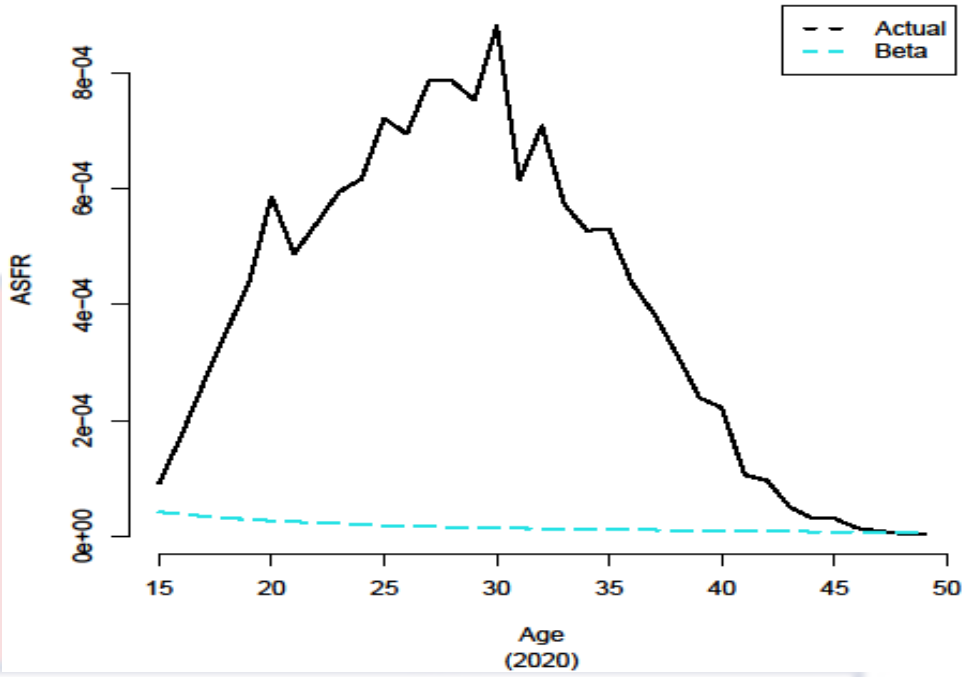

Plots of fitted Beta model and actual ASFRs for the years 2014 – 2020 of Ghana